Efficient Inner-Outer Decoupling Scheme for Non-probabilistic Model Updating with High Dimensional Model Representation and Chebyshev Approximation

Jiang Mo[1], Wang-Ji Yan[1,2*], Ka-Veng Yuen[1,2], Michael Beer[3,4,5]

[1]State Key Laboratory of Internet of Things for Smart City and Department of Civil and Environmental Engineering, University of Macau, China
[2]Guangdong–Hong Kong-Macau Joint Laboratory for Smart Cities, China
[3]Institute for Risk and Reliability, Leibniz Universität Hannover, Hannover 30167, Germany
[4]Institute for Risk and Uncertainty and School of Engineering, University of Liverpool, Liverpool L69 7ZF, UK
[5]International Joint Research Center for Resilient Infrastructure & International Joint Research Center for Engineering Reliability and Stochastic Mechanics, Tongji University, Shanghai 200092, PR China

ABSTRACT: Interval arithmetic offers a powerful tool for structural model updating when uncertain-but-bounded parameters are considered. However, the application of interval model updating for practical engineering structure is hindered due to model complexity and huge computational burden involved in the repeated evaluations of non-probabilistic constraints. In this light, an efficient inner-outer decoupling scheme is proposed for non-probabilistic model updating in this study. The mathematical operation of interval model updating is decomposed into two layers labelled as inner layer with the operation of uncertainty propagation and outer layer with the operation of interval optimization. In the inner uncertainty propagation, the High Dimensional Model Representation (HDMR) is utilized to enable the decomposition of the model outputs in terms of multivariate inputs into the sum of multiple single-variate functions, which is further approximated by Chebyshev polynomials so that the stationary points of each function can be derived. In the outer layer, a fast-running optimization strategy based on the stationary points of Chebyshev polynomial approximation is proposed to accelerate tracking the bounds of model parameters by avoiding time-consuming brute-force interval optimization. As a result, the original non-probabilistic updating process with two interacted layers can be completely decoupled into two independent operations of the inner uncertainty propagation and outer interval optimization so as to enhance the search efficiency and convergence rate significantly. Two numerical case studies illustrate capability of the proposed method in updating the structural parameters intervals efficiently with the model outputs intervals agreeing well with the testing outputs intervals. Two experimental cases of steel plates and the Canton Tower also demonstrates the efficiency and advantages of the method in interval model updating.

Keywords: Finite element model updating; non-probabilistic uncertainty; interval arithmetic; HDMR; polynomial approximation

---

*Corresponding author.

E-mail address: yc17459@um.edu.mo(J. Mo); wangjiyan@um.edu.mo (W.J. Yan)

1 Introduction

In most areas of engineering analysis, physical model plays an important role in characterizing mechanical behavior and helping engineers and researchers to carry out efficient numerical analysis. However, the physical model established based on highly idealized engineering blueprints will inevitably lead to discrepancies from its real counterpart due to modeling simplification and knowledge insufficiency [1-4]. Hence, structural model updating has been an important field in structural and mechanical engineering over the past few decades [1, 5]. Model updating problem usually reduces to minimizing the residuals of structural (static, dynamic and/or modal) outputs between simulated (numerical) structures and corresponding real (experimental) structures [1, 6].

Existing Finite element (FE) model updating methods can be divided into deterministic one and non-deterministic one according to whether uncertainties are properly accommodated and quantified in the updating process [7]. The former regards structural parameters and outputs as deterministic quantities. However, uncertainties always arise in engineering practices due to modeling error, measurement noise and some other factors [8-11]. Ignoring these uncertainties may lead to erroneous results in structural model updating. Therefore, non-deterministic approaches will be necessary if one considers the uncertainties properly. The non-deterministic methods are usually further classified as probabilistic model updating and non-probabilistic model updating [12, 13]. Although probabilistic model updating [14, 15] have been studied extensively with fruitful outcomes, these methods still heavily rely on sufficiency of sample data and empirical hypotheses. In this light, non-probabilistic interval uncertainty [16-18] has been increasingly used to quantify the uncertainties in the fields of mechanical and structural engineering [18-23] since it requires only the boundaries of the uncertain variables with limited samples.

In recent years, a number of interval model updating approaches have been proposed. Khodaparast et al. [24, 25] used Kriging predictor as the meta-model to map the parameters hypercube to the response samples. The interval updating was conducted by continuously adjusting the hypercube and comparing the derived points with experiment samples. This method is relatively complex, and the construction of the Kriging predictor has some limitations. Fang et al. [26] constructed an interval response surface using quadratic polynomials without cross terms, then the model was updated using optimization methods. This approach is clear and easy to implement. Deng et al. [27] proposed an interval model updating method based on perturbation method and radial basis function neural networks used as a surrogate model. This method only applies to small parameter variations and the construction of neural networks is based on experience and trial. Zheng et al. [28] employed universal grey mathematics to construct a novel interval objective function, and gaussian process regression model is used as the surrogate model. The interval upper bounds and interval diameters are updated respectively. This method is applicable for nonlinear monotonic problems.

In addition to abovementioned surrogate based methods, a new method using the concept of interval overlap ratio which describes the consistence object intervals was proposed [29]. The uncertainty propagation was achieved by Monte Carlo simulation. It has high accuracy due to Monte Carlo simulation, but also brings unaffordable computation costs at the same time. Based on sub-interval similarity, Zhao et al. [30] developed an updating strategy considering the range and distributed positions of the intervals. The method can be used in interval and probabilistic model updating. Faes et.al. [31-33] developed an efficient interval optimization method in terms of linear systems based on operator norm theory. Recently, non-probabilistic correlation [34, 35] has been considered in non-probabilistic model updating. Liao et al. [36] and Ouyang et al. [37, 38] applied non-probabilistic correlation propagation technique to model updating and obtained not only the interval bounds of the updating parameters, but also the correlation matrix of the updating parameters. Additionally, interval techniques have been extensively utilized in load identification [39, 40], structural identification and inversion [41, 42], which are closely related to structural model updating.

While these aforementioned interval model updating algorithms provide promising performance on some engineering problems, they are still likely to perform poorly regarding computational efficiency and accuracy due to the increase of model complexity and the complex nature of interval optimization. Therefore, this paper proposes a new inner-outer decoupling scheme to enhance the computational efficiency and improve the performance of existing interval model updating algorithms based on High Dimensional Model Representation (HDMR) and Chebyshev polynomial approximation. The main scientific contribution of this study includes:

- The mathematical operation of interval model updating comprising two interacted layers labelled as inner layer with the operation of uncertainty propagation and outer layer with the operation of interval optimization can be completely decoupled into two independent layers.

- In the inner operation of uncertainty propagation, the multivariate model output functions are decomposed into the sum of multiple single-variate functions utilizing HDMR, and their stationary points are derived based on Chebyshev polynomial approximation.
- In the outer operation of interval optimization, a fast-running optimization strategy based on the stationary points of Chebyshev polynomial approximation is proposed to enhance the search efficiency and convergence capacity significantly.

The organization of this paper is given as follows. Section 2 gives the problem description and basic introduction to interval mathematics. Section 3 illustrates the structural interval model updating strategy with special emphasis on structural interval uncertainty propagation with HDMR and interval optimization based on stationary points of polynomial approximation. Section 4 presents the implementation procedures of the proposed novel decoupling scheme for interval model updating. In Section 5, four cases are investigated as numerical validation and experimental verification for the method.

2 Problem Description

In this section, some general concepts of interval uncertainty [17] are firstly introduced as preliminaries. Then, the fundamentals of interval model updating is given. Finally, some critical challenging issues are also presented.

2.1 Preliminaries of interval uncertainty

Generally speaking, uncertainties can be divided into aleatory uncertainty and epistemic uncertainty [43]. The former is caused by intrinsic randomness, whereas the latter is usually caused by lack of knowledge and insufficient information. Interval uncertainty analysis is useful in epistemic uncertainty quantification with limited information. The primary concern of this study is to consider the non-probabilistic interval method to quantify the epistemic uncertainty caused by information insufficiency in model updating, which applies to cases that insufficient experimental samples are provided. The interval model updating can serve as a supplement to probabilistic model updating.

Let $I\left(\boldsymbol{R}\right)$ and $I\left(\boldsymbol{R}^n\right)$ denote the sets of all real-valued closed intervals and real-valued interval vectors (each element of the vectors is a closed interval), where n denotes the dimension of vectors. Any interval number x^I and interval vector $\boldsymbol{x}^I$ are members of $I\left(\boldsymbol{R}\right)$ and $I\left(\boldsymbol{R}^n\right)$, respectively. The superscript I denotes interval numbers.

For an uncertain variable h, it is bounded in interval mathematics as:

$$h \in h^I = \left[\underline{h}, \overline{h} \right] \tag{1}$$

where $\underline{h}$ and $\overline{h}$ are its lower and upper bounds, respectively.

For an uncertain vector $\boldsymbol{h} = \left(h_1, h_2, \ldots, h_n \right)$ in R^n, it is bounded as:

$$\boldsymbol{h} \in \boldsymbol{h}^I = \left(h_1{}^I, h_2{}^I, \ldots, h_n{}^I \right) \tag{2}$$

where each element of $\boldsymbol{h}^I$ belongs to $I\left(\boldsymbol{R}\right)$, namely,

$$h_i{}^I = \left[\underline{h}_i, \overline{h}_i \right] \quad \left(i = 1, 2, \cdots, n \right) \tag{3}$$

Apart from interval bounds, interval numbers can be denoted by their interval midpoints (interval centers) h_i^c and interval radius $\Delta h_i \left(i = 1, 2, \cdots, n \right)$. The interval midpoints and radius are defined as:

$$h_i^c = \frac{\overline{h}_i + \underline{h}_i}{2}, \quad \Delta h_i = \frac{\overline{h}_i - \underline{h}_i}{2} \quad \left(i = 1, 2, \cdots, n \right) \tag{4}$$

To avoid confusions, it is worth noting that the notation "Δx" is used to denote interval radius in this study, whereas it means the difference between the measurement result and the actual value in measurement practice.

Then, h_i^I can be rearranged as following usable form:

$$h_i{}^I = \left[h_i^c - \Delta h_i, h_i^c + \Delta h_i \right] = h_i^c + e \cdot \Delta h_i \quad \left(i = 1, 2, \cdots, n \right) \tag{5}$$

where $e = \left[-1, 1 \right]$. For the uncertain parameter vector $\boldsymbol{h} \in \boldsymbol{h}^I$, it can be written as:

$$\boldsymbol{h} = \boldsymbol{h}^c + \boldsymbol{t} \circ \Delta \boldsymbol{h} \tag{6}$$

where $\boldsymbol{h}^c = \left(h_1^c, h_2^c, \ldots, h_n^c \right)$; $\Delta \boldsymbol{h} = \left(\Delta h_1, \Delta h_2, \ldots, \Delta h_n \right)$; $\boldsymbol{t}$ is a vector whose elements are within the interval $\left[-1, 1 \right]$; and '$\circ$' denotes the element-wise product (which is also known as Hadamard product).

2.2 Fundamentals of interval model updating

Compared with deterministic model updating in which the structural model outputs and physical parameters are viewed as real numbers, interval model updating regards the structural model outputs and physical parameters as interval numbers. The aim of interval model updating is to calibrate the bounds of the structural interval parameters in order that the theoretical interval outputs of the structure will be consistent with the testing interval outputs.

For a structural system, let $\boldsymbol{p} = \{p_i\}(i = 1, 2, \cdots, m)$ denote a vector with m uncertain physical parameters to be updated, while the vector $\boldsymbol{Y} = \{Y_j\}(j = 1, 2, \cdots, s)$ represents s structural model outputs given $\boldsymbol{p}$. If the uncertain parameters $\boldsymbol{p}$ are interval numbers with insufficient information, then the theoretical outputs $\boldsymbol{Y}$ will also be interval numbers. Likewise, if the testing outputs $\boldsymbol{Y}^e$ are interval numbers, the identified structural parameters will also be interval numbers. It is assumed that the structural model outputs $\boldsymbol{Y}$ are continuous with respect to the physical parameters $\boldsymbol{p}$. Since $\boldsymbol{p}$ is a continuous closed interval vector, the function $\boldsymbol{Y}(\boldsymbol{p})$ will form a continuous closed interval as well considering the continuity of $\boldsymbol{Y}(\boldsymbol{p})$. In this context, the mathematical problem of interval model updating is given as:

$$\begin{aligned}
&\textit{find} && \underline{\boldsymbol{p}}, \overline{\boldsymbol{p}} \\
& && \underline{p}_i, \overline{p}_i \left(i = 1, 2, \cdots, m\right) \\
&\text{minimize} && \sum_{j=1}^{s} \left| \frac{\overline{Y}_j\left(\underline{\boldsymbol{p}}, \overline{\boldsymbol{p}}\right) - \overline{Y}_j^e}{\overline{Y}_j^e} \right| + \sum_{j=1}^{s} \left| \frac{\underline{Y}_j\left(\underline{\boldsymbol{p}}, \overline{\boldsymbol{p}}\right) - \underline{Y}_j^e}{\underline{Y}_j^e} \right| \\
&s.t. && \boldsymbol{LB} \le \underline{\boldsymbol{p}} \le \overline{\boldsymbol{p}} \le \boldsymbol{UB}
\end{aligned} \tag{7}$$

where $\underline{p}_i, \overline{p}_i \left(i = 1, 2, \cdots, m\right)$ denote the lower and upper bounds of the i-th physical parameter to be updated; $\boldsymbol{LB}, \boldsymbol{UB}$ denote the parameter optimization bounds of $\underline{\boldsymbol{p}}, \overline{\boldsymbol{p}}$; $\underline{Y}_j\left(\underline{\boldsymbol{p}}, \overline{\boldsymbol{p}}\right), \overline{Y}_j\left(\underline{\boldsymbol{p}}, \overline{\boldsymbol{p}}\right)\left(j = 1, 2, \cdots, s\right)$ denote the simulated lower and upper bounds of the structural model outputs with interval parameters $\boldsymbol{p}^I = \left[\underline{\boldsymbol{p}}, \overline{\boldsymbol{p}}\right]$; $\underline{Y}_j^e, \overline{Y}_j^e \left(j = 1, 2, \cdots, s\right)$ are the real upper and lower bounds of the j-th structural model output.

It is worth mentioning that the structural parameters to be updated in Eq. (7) should be positive. The absolute value of the relative errors is utilized in the objective function considering that the relative error can balance the contributions of the upper bounds $\overline{Y}_j\left(\underline{\boldsymbol{p}}, \overline{\boldsymbol{p}}\right)$ and lower bounds $\underline{Y}_j\left(\underline{\boldsymbol{p}}, \overline{\boldsymbol{p}}\right)$ of the objective function. Furthermore, the L1 norm is more robust to outliers compared to the L2 norm since it increases the cost of outliers linearly. If the chosen response Y is very close to 0, the relative error may not be suitable and another criterion such as absolute error and mean square error should be utilized.

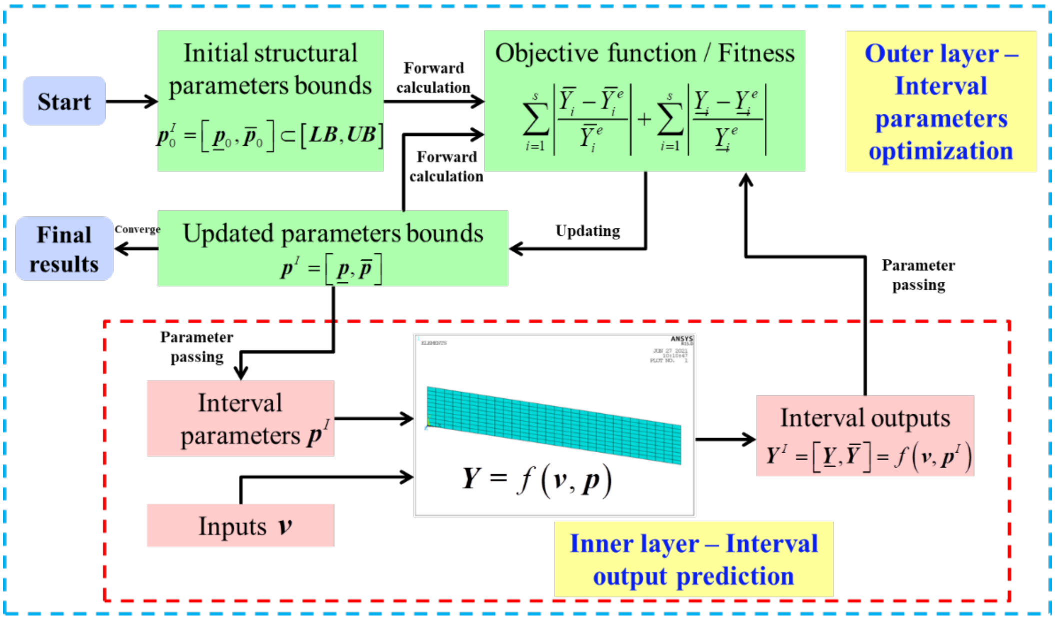

Figure 1: Illustration of the fundamental procedures and mathematical operation of conventional interval model updating algorithms

It is worth noting that the interval model updating procedures mentioned in the above reduces to an optimization problem shown in Eq. (7). In this study, for the convenience of further illustration, the mathematical operation of interval model updating is investigated and one can figure out that it can be decomposed into two layers as shown in Figure 1. One layer is labelled as the inner layer with the operation of uncertainty propagation from the interval structural parameters to the interval structural outputs. As a forward problem, the inner layer aims to calculate the stationary points and interval bounds of the outputs $\underline{Y}_i, \overline{Y}_i$ with specified interval physical parameters $\underline{p}_i, \overline{p}_i$. The other layer is labelled as the outer layer with the operation of interval optimization, which aims to search the optimal bounds so as to update $\underline{p}_i, \overline{p}_i$ by minimizing the residual function in Eq. (7).

The outer layer requires to calculate the interval bounds $\boldsymbol{Y}^I = \left[\underline{\boldsymbol{Y}}, \overline{\boldsymbol{Y}}\right]$ of the structural outputs $\boldsymbol{Y}(\boldsymbol{p})$ given $\underline{\boldsymbol{p}}, \overline{\boldsymbol{p}}$ in each optimization updating step. In other words, the inner layer of uncertainty propagation will be implemented each time when we update the parameters bounds $\underline{\boldsymbol{p}}, \overline{\boldsymbol{p}}$ in the outer layer of bound optimization process, which is repetitive and time consuming. To address this issue, an updating strategy of the stationary points is proposed in this study.

2.3 Challenges and strategies

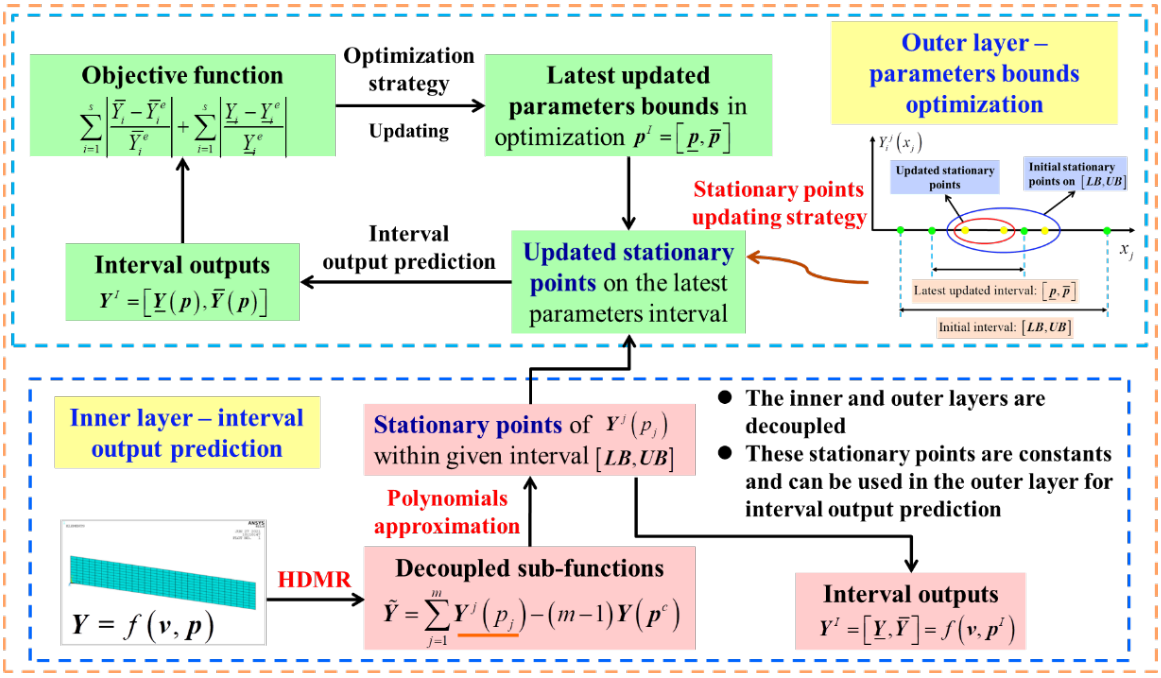

Figure 2: Schematic diagram of the interval model updating using the inner-outer-decoupling scheme

Although significant progress has been achieved for interval model updating, there are still some challenges which hinder its practical implementation:

- In the conventional interval model updating methods, the inner layer and outer layer are usually interacting with one another. In the other words, in the outer layer of bounds optimization for structural physical parameters, repetitive searches of optimal points are required in each iteration step since the inner layer of uncertainty propagation analysis is always required in this problem immediately after an updated interval $\left[\underline{p}_i, \overline{p}_i\right]$ is given. Hence, how to trade off the computation cost and accuracy deserves further investigation.
- To reduce the computational burden involved in the interval model updating due to repeating runs of finite element model analysis package with any parameter update, fast-running metamodels that approximate multivariate input/output relationships have been used to replace the time-consuming physical-based computer models. However, the inner and outer layers are coupled in existing surrogate model-based interval model updating which requires repetitive evaluations of the interval structural outputs. Furthermore, non-intrusive interval algorithms encounter challenges such as complex model construction and high computational costs. Neural networks based surrogate models requires a large number of training samples, manual adjustment which may be problem-specific.
- For the inner layer uncertainty propagation problem, various approaches such as

perturbation method, series expansion method, Monte Carlo simulation and optimization methods have been used and have achieved satisfactory effects. However, the perturbation and series expansion methods require that the intervals are narrow, and they have uncontrollable errors when the surrogate model is nonlinear or when the variable intervals are relatively wide. Monte Carlo simulation and optimization methods suffer from high computational efforts.

To address these problems, we will utilize the HDMR to decompose the multivariate structural output function into several single-variate functions, which reduces the dimensionality and, hence, the difficulty of the inner uncertainty propagation. Then, Chebyshev polynomial functions are employed to approximate each single-variate function and its stationary points are analytically obtained within the given parameter optimization bounds. For the outer interval optimization, an efficient stationary points updating strategy is proposed without repetitive searching of optimal points on the updated intervals. In this study, HDMR helps to solve the stationary points of the structural output functions within the specified parameter optimization bounds $\left[\boldsymbol{LB},\boldsymbol{UB}\right]$ in the inner layer, and these stationary points are constants which can be directly used for output interval prediction required in the outer interval optimization. As a result, the non-probabilistic updating can be decoupled into two independent operations of the inner uncertainty propagation and outer interval optimization which are interacted with each other in the original problem. Figure 2 shows the solution strategy by decoupling two-layer in Figure 1.

3 Inner-outer-decoupling Scheme for Interval Model Updating

In this study, the structural interval model updating is achieved based on two main strategies. HDMR is firstly utilized for decomposing the multivariate functions into the sum of multiple single-variate functions. To alleviate the computational burden of the interval optimization, Chebyshev polynomial approximation is adopted to determine the stationary points of the functions of interest (i.e., the first-order derivatives of the functions are zero).

3.1 Multivariate function decomposition with HDMR for inner uncertainty propagation

High dimensionality is one of the main obstacles in many engineering fields. Structural model updating also usually suffer from the curse of dimension. The HDMR theory proposed by Rabitz et al. [44] is widely recognized as an effective way and has been used in mechanical engineering [45, 46]. A brief review of relevant theories is given as follows.

For an input-output system $f(\boldsymbol{x}) = f(x_1, \ldots, x_m)$ within domain Ω, the following expression is used to represent it by summands with various dimensions:

$$f(\boldsymbol{x}) = f_0 + \sum_{i=1}^{m} f_i(x_i) + \sum_{1 \le i < j \le m}^{m} f_{ij}(x_i, x_j) + \sum_{1 \le i < j < k \le m}^{m} f_{ijk}(x_i, x_j, x_k) + \cdots + f_{12\cdots m}(x_1, \ldots, x_m) \tag{8}$$

where f_0 is a constant; $f_i(x_i)$ denotes the individual contribution to $f(\boldsymbol{x})$ of each variable, and the rest of the terms are the joint contribution of these variables on $f(\boldsymbol{x})$.

It has been widely reported that the approximation is usually dominated by the low-order correlation terms only. Therefore, the first-order expression can usually achieve acceptable results in engineering practices. A concrete expression of Eq. (8) is required in real applications. Cut-HDMR is a useful expression of Eq. (8), which expresses $f(\boldsymbol{x})$ in terms of a specific reference point $\overline{\boldsymbol{x}}$ in domain Ω. The component functions ($f_0, f_i(x_i), f_{ij}(x_i, x_j), \cdots$) of cut-HDMR with respect to $\overline{\boldsymbol{x}}$ are given as follows:

$$\begin{gathered} f_0 = f(\overline{\boldsymbol{x}}) \\ f_i(x_i) = f(x_i, \overline{\boldsymbol{x}}^i) - f_0 \\ f_{ij}(x_i, x_j) = f(x_i, x_j, \overline{\boldsymbol{x}}^{ij}) - f_i(x_i) - f_j(x_j) - f_0 \\ \cdots \end{gathered} \tag{9}$$

where $(x_i, \overline{\boldsymbol{x}}^i)$ and $(x_i, x_j, \overline{\boldsymbol{x}}^{ij})$ are equal to $(\overline{x}_1, \ldots, \overline{x}_{i-1}, x_i, \overline{x}_{i+1}, \ldots, \overline{x}_m)$ and $(\overline{x}_1, \ldots, \overline{x}_{i-1}, x_i, \overline{x}_{i+1}, \ldots, \overline{x}_{j-1}, x_j, \overline{x}_{j+1}, \ldots, \overline{x}_m)$, respectively. Herein, the first order cut-HDMR will be given as a special case. Its advantage on interval model updating will be elaborated in Section 3.2.

Given a function $f(\boldsymbol{x}) = f(x_1, \ldots, x_m)$ with physical parameter intervals $\boldsymbol{x} \in \boldsymbol{x}^I = [\underline{\boldsymbol{x}}, \overline{\boldsymbol{x}}]$, and a reference point $\boldsymbol{x}^0 = (x_1^0, x_2^0, x_3^0, \ldots, x_m^0)^T$ on interval $\boldsymbol{x}^I = [\underline{\boldsymbol{x}}, \overline{\boldsymbol{x}}]$, the function can be approximated using HDMR decomposition by:

$$\begin{aligned} \tilde{f}(\boldsymbol{x}) &= f(x_1, x_2^0, x_3^0, \ldots, x_m^0) + f(x_1^0, x_2, x_3^0, \ldots, x_m^0) + \cdots + f(x_1^0, x_2^0, x_3^0, \ldots, x_m) - (m-1) f(\boldsymbol{x}^0) \\ &= \sum_{i=1}^{m} f_i(x_i) - (m-1) f(\boldsymbol{x}^0) \end{aligned} \tag{10}$$

where $f_i(x_i) = f(x_1^0, x_2^0, \ldots, x_i, \ldots, x_m^0)$.

Taking the first-order Taylor expansion of functions $f_i(x_i)$ and $f(\boldsymbol{x})$ at the reference points $x_i^0, \boldsymbol{x}^0$ respectively, one has:

$$f_i\left(x_i\right)=f_i\left(x_i^0\right)+\frac{df_i}{dx_i}\left(x_i-x_i^0\right)+o\left(x_i-x_i^0\right)=f\left(\boldsymbol{x}^0\right)+\frac{df_i}{dx_i}\left(x_i^0\right)\delta x_i+R_{f_{sub}}\left(\delta x_i\right) \tag{11}$$

and

$$f\left(\boldsymbol{x}\right)=f\left(\boldsymbol{x}^0\right)+\sum_{i=1}^{m}\frac{\partial f}{\partial x_i}\left(x_i-x_i^0\right)=f\left(\boldsymbol{x}^0\right)+\sum_{i=1}^{m}\frac{\partial f}{\partial x_i}\delta x_i+R_f\left(\delta\boldsymbol{x}\right) \tag{12}$$

where $\delta x_i=x_i-x_i^0$, and the Lagrange form of the remainders $R_{f_{sub}}\left(\delta x_i\right)$ and $R_f\left(\delta\boldsymbol{x}\right)$ are given by:

$$R_{f_{sub}}\left(\delta x_i\right)=\frac{f_i''(\xi_i)}{2!}\left(\delta x_i\right)^2 \quad , \quad \xi_i \text{ is between } x_i^0 \text{ and } x_i \tag{13}$$

and

$$R_f\left(\delta\boldsymbol{x}\right)=\frac{1}{2}\left(\left(\delta x_1\right)\frac{\partial}{\partial x_1}+\left(\delta x_2\right)\frac{\partial}{\partial x_2}+\cdots+\left(\delta x_m\right)\frac{\partial}{\partial x_m}\right)^2 f\left(\boldsymbol{\zeta}\right) \quad , \quad \boldsymbol{\zeta} \text{ is between } \boldsymbol{x}^0 \text{ and } \boldsymbol{x} \tag{14}$$

For ease of clarity, let $R_{f_{sub}}\left(\delta\boldsymbol{x}\right)=\sum_{i=1}^{m}R_{f_{sub}}\left(\delta x_i\right)$.

Then, we obtain the error of the HDMR decomposition:

$$\begin{aligned}
error &= \tilde{f}\left(\boldsymbol{x}\right)-f\left(\boldsymbol{x}\right)\\
&=\left[\sum_{i=1}^{m}f_i\left(x_i\right)-\left(m-1\right)f\left(\boldsymbol{x}^0\right)\right]-f\left(\boldsymbol{x}\right)\\
&=\left[\sum_{i=1}^{m}f_i\left(x_i\right)-\left(m-1\right)f\left(\boldsymbol{x}^0\right)\right]-\left[f\left(\boldsymbol{x}^0\right)+\sum_{i=1}^{m}\frac{\partial f}{\partial x_i}\delta x_i+R_f\left(\delta\boldsymbol{x}\right)\right]\\
&=\sum_{i=1}^{m}\left[f_i\left(x_i\right)-f\left(\boldsymbol{x}^0\right)\right]-\sum_{i=1}^{m}\frac{\partial f}{\partial x_i}\delta x_i-R_f\left(\delta\boldsymbol{x}\right)\\
&=\sum_{i=1}^{m}\left[\frac{df_i}{dx_i}\left(x_i^0\right)\delta x_i+R_{f_{sub}}\left(\delta x_i\right)\right]-\sum_{i=1}^{m}\frac{\partial f}{\partial x_i}\delta x_i-R_f\left(\delta\boldsymbol{x}\right)\\
&=\sum_{i=1}^{m}R_{f_{sub}}\left(\delta x_i\right)-R_f\left(\delta\boldsymbol{x}\right)\\
&=R_{f_{sub}}\left(\delta\boldsymbol{x}\right)-R_f\left(\delta\boldsymbol{x}\right)
\end{aligned} \tag{15}$$

As is seen in Eq. (15), when $\boldsymbol{x}\to\boldsymbol{x}^0\left(\delta\boldsymbol{x}\to\boldsymbol{0}\right)$, the error is approaching 0. That is to say, the error will be small provided that the interval width is not too large.

According to above analysis, the cut-HDMR can represent the original function in the vicinity of the reference point. In addition, it has the advantage of decomposing multivariate functions into the sum of multiple single-variate functions, bringing conveniences to the implementation of the inner layer with the operation of uncertainty propagation in the procedure of model updating. Hence, the cut-HDMR is applied to represent structural theoretical outputs in this study.

The structural theoretical output $\boldsymbol{Y}$ is a vector function of the structural physical parameter vector $\boldsymbol{p}$, i.e., $\boldsymbol{Y}=\boldsymbol{Y}(\boldsymbol{p})$. The interval midpoint of $\boldsymbol{p}^I=\left[\underline{\boldsymbol{p}},\overline{\boldsymbol{p}}\right]$ is $\boldsymbol{p}^c$. Based on the HDMR formula in Eq. (10), the theoretical output vector can be approximately represented as:

$$\tilde{\boldsymbol{Y}}=\sum_{j=1}^{m}\boldsymbol{Y}^j\left(p_j\right)-(m-1)\boldsymbol{Y}\left(\boldsymbol{p}^c\right) \tag{16}$$

where $\boldsymbol{p}^c$ is taken as the reference point.

The *i*-th entry of $\tilde{\boldsymbol{Y}}$ is given by:

$$\tilde{Y}_i=\sum_{j=1}^{m}Y_i^j\left(p_j\right)-(m-1)Y_i\left(\boldsymbol{p}^c\right) \tag{17}$$

where $Y_i\left(\boldsymbol{p}^c\right)$ is a constant representing the *i*-th structural output at the interval midpoint $\boldsymbol{p}^c$.

As was mentioned in Section 2.2, one important problem in Eq. (7) is to calculate the bound of the outputs $\boldsymbol{Y}^I=\left[\underline{\boldsymbol{Y}},\overline{\boldsymbol{Y}}\right]=\left[\underline{Y}_i\left(\underline{\boldsymbol{p}},\overline{\boldsymbol{p}}\right),\overline{Y}_i\left(\underline{\boldsymbol{p}},\overline{\boldsymbol{p}}\right)\middle| i=1,2,\cdots,s\right]$ based on the given interval physical parameters $\boldsymbol{p}^I=\left[\underline{\boldsymbol{p}},\overline{\boldsymbol{p}}\right]$. This can be regarded as a problem of structural interval output prediction described by:

$$\begin{aligned}\overline{\boldsymbol{Y}}(\boldsymbol{p})&=\max_{\boldsymbol{p}\in\boldsymbol{p}^I}\boldsymbol{Y}(\boldsymbol{p})\\ \underline{\boldsymbol{Y}}(\boldsymbol{p})&=\min_{\boldsymbol{p}\in\boldsymbol{p}^I}\boldsymbol{Y}(\boldsymbol{p})\end{aligned} \tag{18}$$

The vector $\boldsymbol{Y}=\boldsymbol{Y}(\boldsymbol{p})$ consists of s structural outputs. Each entry of Eq. (18) is:

$$\begin{cases}\overline{Y}_i(\boldsymbol{p})=\max\limits_{\boldsymbol{p}\in\boldsymbol{p}^I}Y_i(\boldsymbol{p})\\ \underline{Y}_i(\boldsymbol{p})=\min\limits_{\boldsymbol{p}\in\boldsymbol{p}^I}Y_i(\boldsymbol{p})\end{cases}\quad(i=1,2,\cdots,s) \tag{19}$$

Without loss of generality, the *i*-th theoretical model output Y_i is taken as an example. The interval prediction problem becomes a problem of searching for function extreme values in Eq. (19). According to Eq. (17), the m-variate function Y_i can be approximated by the sum of *m* single-variate functions $Y_i^j\left(p_j\right)(j=1,2,\cdots,m)$. As a result, Eq. (19) can be transformed as:

$$\begin{cases} \max\limits_{p_j \in [\underline{p}_j, \overline{p}_j]} Y_i^j(p_j) \\ \min\limits_{p_j \in [\underline{p}_j, \overline{p}_j]} Y_i^j(p_j) \end{cases} \quad (i = 1, 2, \cdots, s \ , \ j = 1, 2, \cdots, m) \tag{20}$$

The structural output interval prediction can be solved when the interval bounds of each single-variate function $Y_i^j(p_j)$ is achieved. The advantages of application of Eq. (17) and Eq. (20) to the following sections will indicate that the decomposition of multivariate model input/output function into multiple single-variate functions will significantly reduce the computational costs and simplify the original function.

3.2 Chebyshev polynomial approximation for $Y_i^j(p_j)$ and its stationary points

As was mentioned in the last section, one should solve the interval of $Y_i^j(p_j)$ in the procedure of interval optimization with each parameter updated. Since the explicit form of $Y_i^j(p_j)$ is unknown, numerical optimization or intelligent optimization algorithms should be used to solve Eq. (20). To calculate the extreme points and corresponding values of $Y_i^j(p_j)$ more efficiently, the strategy of function approximation will be employed. Chebyshev polynomials as a powerful tool to approximate functions have been used in a wide range of engineering problems [47-49]. Therefore, $Y_i^j(p_j)$ is approximated by using the Chebyshev polynomials in this study. Then, the problem of solving the bounds of $Y_i^j(p_j)$ reduces to solve the maximum and minimum values of a much simpler function. For this purpose, the first-class Chebyshev polynomials are introduced:

$$T_n(x) = \cos(n \arccos x), \quad x \in [-1, 1] \tag{21}$$

where n is a nonnegative integer; $\{T_n(x)\}$ constitutes Chebyshev polynomials series, which can also be obtained using the following recursive formula:

$$\begin{cases} T_0(x) = 1, \\ T_1(x) = x, \\ T_{n+1}(x) = 2xT_n(x) - T_{n-1}(x) \end{cases} \quad (n = 1, 2, 3, \cdots) \tag{22}$$

For any function $f(x)$ defined on interval $[-1, 1]$, it can be represented by $p_r(x)$ with $\mathrm{Span}\{T_0, T_1, \ldots, T_r\}$, i.e., the r-th order approximation polynomial $H_r(x)$ of $f(x)$ is equal to:

$$H_r\left(x\right)=\frac{t_0}{2}+\sum_{j=1}^{r}t_jT_j\left(x\right) \tag{23}$$

Eq. (23) is an approximation of $f\left(x\right)$, and the coefficients are given by:

$$\begin{cases} t_0=\dfrac{2}{\pi}\displaystyle\int_{-1}^{1}\frac{f\left(x\right)}{\sqrt{1-x^2}}\mathrm{d}x, \\ t_j=\dfrac{2}{\pi}\displaystyle\int_{-1}^{1}\frac{f\left(x\right)T_j\left(x\right)}{\sqrt{1-x^2}}\mathrm{d}x \end{cases} \quad \left(j=1,2,\cdots,r\right) \tag{24}$$

Eq. (24) can be calculated according to Gauss-Chebyshev quadrature formula:

$$\begin{cases} t_0=\dfrac{2}{\pi}\displaystyle\int_{-1}^{1}\frac{f\left(x\right)}{\sqrt{1-x^2}}\mathrm{d}x\approx\sum_{k=1}^{q}A_kf\left(x_k\right), \\ t_j=\dfrac{2}{\pi}\displaystyle\int_{-1}^{1}\frac{f\left(x\right)T_j\left(x\right)}{\sqrt{1-x^2}}\mathrm{d}x\approx\sum_{k=1}^{q}A_kf\left(x_k\right)T_j\left(x_k\right) \end{cases} \quad \left(j=1,2,\cdots,r\right) \tag{25}$$

where $x_k\left(k=1,2,\cdots,q\right)$ at the q quadrature nodes are determined by:

$$x_k=\cos\frac{2\left(q-k\right)+1}{2q}\pi \quad \left(k=1,2,\cdots,q\right) \tag{26}$$

It should be mentioned that $f\left(x_k\right)$ in Eq. (25) is the structural output value at the collocation point x_k, and the q quadrature coefficients are calculated by:

$$A_k=\int_{-1}^{1}\frac{T_q\left(x\right)}{\sqrt{1-x^2\left(x-x_k\right)T_q'\left(x_k\right)}}\mathrm{d}x=\frac{\pi}{q} \quad \left(k=1,2,\cdots,q\right) \tag{27}$$

Then, the approximation of $f\left(x\right)$ is obtained as follows:

$$H_r\left(x\right)=\frac{1}{q}\sum_{k=1}^{q}f\left(x_k\right)+\frac{2}{q}\sum_{j=1}^{r}\sum_{k=1}^{q}f\left(x_k\right)T_j\left(x_k\right)T_j\left(x\right) \tag{28}$$

In terms of the numerical error of the Chebyshev polynomial approximation, a high order Chebyshev polynomial series can effectively reduce the approximation error [47]. Hence, adopting a high order (usually 3 or 4) Chebyshev polynomial can guarantee the precision requirement for the settings of the polynomial approximation.

Since $f\left(x\right)$ has been replaced by Eq. (28) with explicit expression, the stationary points of $f\left(x\right)$ are easily obtained by taking a derivative of Eq. (28) as follow:

$$H_r'(x)=\frac{2}{q}\sum_{j=1}^{r}\sum_{k=1}^{q} f(x_k)T_j(x_k)T_j'(x)=0 \tag{29}$$

For $Y_i^j(p_j)$ with $p_j \in [\underline{p}_j, \overline{p}_j](j=1,2,\cdots,m)$, the midpoint-radius notation in Eq. (5) is utilized to normalize the variable p_j to interval $[-1,1]$:

$$p_j = p_j^c + \Delta p_j \cdot x_j \quad , \quad x_j \in [-1,1] \tag{30}$$

Regarding $Y_i^j(p_j)=Y_i^j(x_j)$ as $f(x)$, the stationary points of $Y_i^j(p_j)$ is similarly solved and marked as:

$$\{x_{j,d}\}=\left\{x_j \middle| Y_i^{j\prime}(x_j)=0, x_j \in [-1,1]\right\} \tag{31}$$

Considering that the extreme values of a continuous function on closed intervals are achieved at the interval endpoints or stationary points, the extreme points of $Y_i^j(p_j)$ are:

$$\begin{aligned} x_{j,\max} &= \left\{x_j \middle| Y_i^j(x_j)=\max\left(Y_i^j\left(\{x_{j,d}\}\right), Y_i^j(-1), Y_i^j(1)\right)\right\} \\ x_{j,\min} &= \left\{x_j \middle| Y_i^j(x_j)=\min\left(Y_i^j\left(\{x_{j,d}\}\right), Y_i^j(-1), Y_i^j(1)\right)\right\} \end{aligned} \tag{32}$$

When j successively takes 1 to *m*, the maximum and minimum points set of the *i*-th output function Y_i can be obtained as follows:

$$\begin{aligned} (\boldsymbol{x}_i)_{\max} &= \{x_{1,\max}, x_{2,\max}, \ldots, x_{m,\max}\} \\ (\boldsymbol{x}_i)_{\min} &= \{x_{1,\min}, x_{2,\min}, \ldots, x_{m,\min}\} \end{aligned} \tag{33}$$

Likewise, when *i* successively takes 1 to *s*, the extreme points of other elements of $\boldsymbol{Y}$ can also be solved in the same way. At this point, all extreme points of $\boldsymbol{Y}$ on intervals $p_j \in [\underline{p}_j, \overline{p}_j](j=1,2,\cdots,m)$ have been obtained dimension by dimension through taking the advantage of the first-order HDMR. One core issue of interval model updating, i.e., the inner layer with the operation of uncertainty propagation from the structural parameters to the outputs, is solved with high efficiency.

In the inner layer, the HDMR is utilized to represent the real structural output functions and Chebyshev polynomial is employed to calculate the stationary points of these output functions within the given optimization bounds $[\boldsymbol{LB}, \boldsymbol{UB}]$. This layer will be performed only once since these stationary points will remain unchanged on interval $[\boldsymbol{LB}, \boldsymbol{UB}]$ in the optimization process of the outer layer. In this sense, the inner and outer layers are decoupled.

3.3 Outer interval optimization based on stationary points of polynomial approximation

In the outer interval bounds optimization, the inner layer of uncertainty propagation will be implemented each time when we update the parameters bounds $\underline{\boldsymbol{p}}, \overline{\boldsymbol{p}}$ in the outer layer of bound optimization process to calculate the interval bounds $\boldsymbol{Y}^I = \left[\underline{\boldsymbol{Y}}, \overline{\boldsymbol{Y}}\right]$ of the structural outputs $\boldsymbol{Y}\left(\boldsymbol{p}\right)$ given $\underline{\boldsymbol{p}}, \overline{\boldsymbol{p}}$, which is repetitive and time consuming. To address this issue, an updating strategy of the stationary points is proposed here.

According to Section 3.2, the stationary points are of great significance since the model input-output functions always achieve their extreme values at the interval endpoints or stationary points within the interval. Hence, determining structural output bounds is equivalent to solve their stationary points. Fortunately, the proposed HDMR-assisted decoupling scheme for interval model updating has the advantage on tracking the stationary points with the aid of Chebyshev polynomial.

In the proposed interval model updating method, the optimization bounds $\left[\boldsymbol{LB}, \boldsymbol{UB}\right]$ of the physical parameters are fixed. Hence, the stationary points of the structural outputs on the interval $\left[\boldsymbol{LB}, \boldsymbol{UB}\right]$ will be fixed. Once the stationary points of the structural outputs are obtained in the inner layer, the inner and outer layers are separated completely since these stationary points are constants and they will be used to evaluate the extreme values of the structural outputs in the outer layer.

The rationale of interval optimization strategy by making full use of the stationary points is schematically explained in Figure 3. Detailed illustrations are given in the following part of this section.

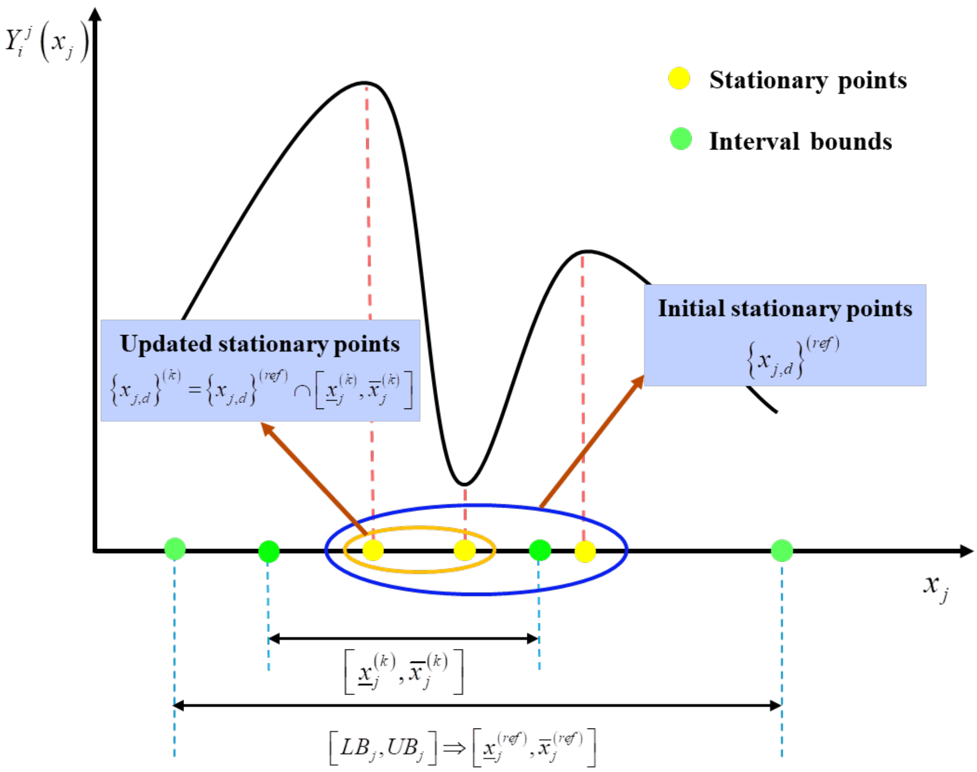

Figure 3: Illustration of the updating of stationary points in the optimization process

For Eq. (7), the lower and upper bounds $\boldsymbol{LB}, \boldsymbol{UB}$ are usually predefined in various optimization algorithms. The interval $[\boldsymbol{LB}, \boldsymbol{UB}]$ should be specified reasonably according to experiences and numerical analysis. Suppose that in initial optimization step marked by ref, the structural interval parameter is the given lower and upper bounds of the optimization parameters $\boldsymbol{p} \in \left[\underline{\boldsymbol{p}}^{(ref)}, \overline{\boldsymbol{p}}^{(ref)}\right] = [\boldsymbol{LB}, \boldsymbol{UB}]$. It can be normalized to $[\mathbf{-1}, \mathbf{+1}]$ through transformation:

$$p_j^{(ref)} = \left(p_j^c\right)^{(ref)} + \Delta p_j^{(ref)} \cdot x_j^{(ref)} \quad , \quad x_j^{(ref)} \in [-1,1] \\ (j = 1, 2, \cdots, m) \tag{34}$$

The stationary points of $Y_i^j(p_j) = Y_i^j(x_j)$ on the interval $[-1,1]$ are:

$$\{x_{j,d}\}^{(ref)} = \left\{x_j^{(ref)} \middle| Y_i^{j\prime}\left(x_j^{(ref)}\right) = 0, x_j^{(ref)} \in [-1,1]\right\} \tag{35}$$

It should be noted that the initial/reference stationary points of the structural output functions in Eq. (35) are obtained on the widest interval $[\boldsymbol{LB}, \boldsymbol{UB}]$ corresponding to the bounds of the optimization parameters $\underline{\boldsymbol{p}}, \overline{\boldsymbol{p}}$. Hence, arbitrary updating of $\underline{\boldsymbol{p}}, \overline{\boldsymbol{p}}$ should be included in this interval, i.e., $\left[\underline{\boldsymbol{p}}, \overline{\boldsymbol{p}}\right] \subset [\boldsymbol{LB}, \boldsymbol{UB}]$. Based on this fact, the stationary points on any updated interval of $\underline{\boldsymbol{p}}, \overline{\boldsymbol{p}}$ in the optimization process can be further achieved, which will be explained as follows.

In any step marked by k during the whole optimization process, an updated interval $\left[\underline{\boldsymbol{p}}^{(k)}, \overline{\boldsymbol{p}}^{(k)}\right] \subset [\boldsymbol{LB}, \boldsymbol{UB}]$ is given based on specific optimization strategy. Note that $p_j^{(k)}$ can also be normalized based on the initial interval $\left[\underline{\boldsymbol{p}}^{(ref)}, \overline{\boldsymbol{p}}^{(ref)}\right]$ as follows:

$$p_j^{(k)} = \left(p_j^c\right)^{(ref)} + \Delta p_j^{(ref)} \cdot x_j^{(k)} \quad , \quad x_j^{(k)} \in [-1,1] \tag{36}$$

Therefore, $\left[\underline{\boldsymbol{p}}^{(k)}, \overline{\boldsymbol{p}}^{(k)}\right]$ is then transformed to the following interval:

$$\left[\underline{x}_j^{(k)}, \overline{x}_j^{(k)}\right] \tag{37}$$

$\underline{x}_j^{(k)}$ and $\overline{x}_j^{(k)}$ satisfy that:

$$\begin{aligned} \underline{p}_j^{(k)} &= \left(p_j^c\right)^{(ref)} + \Delta p_j^{(ref)} \cdot \underline{x}_j^{(k)} \\ \overline{p}_j^{(k)} &= \left(p_j^c\right)^{(ref)} + \Delta p_j^{(ref)} \cdot \overline{x}_j^{(k)} \end{aligned} \tag{38}$$

As Figure 3 shows, in step k, corresponding stationary points of $Y_i^j\left(p_j\right) = Y_i^j\left(x_j\right)$ on interval $[-1,1]$ are directly obtained by:

$$\left\{x_{j,d}\right\}^{(k)} = \left\{x_{j,d}\right\}^{(ref)} \cap \left[\underline{x}_j^{(k)}, \overline{x}_j^{(k)}\right] \tag{39}$$

After obtaining the new stationary points, the extreme points of function $Y_i^j\left(p_j\right) = Y_i^j\left(x_j\right)$ can be easily obtained by:

$$\begin{aligned} x_{j,\max}^{(k)} &= \left\{x_j \middle| Y_i^j\left(x_j\right) = \max\left(Y_i^j\left(\left\{x_{j,d}\right\}^{(k)}\right), Y_i^j\left(\underline{x}_j^{(k)}\right), Y_i^j\left(\overline{x}_j^{(k)}\right)\right)\right\} \\ x_{j,\min}^{(k)} &= \left\{x_j \middle| Y_i^j\left(x_j\right) = \min\left(Y_i^j\left(\left\{x_{j,d}\right\}^{(k)}\right), Y_i^j\left(\underline{x}_j^{(k)}\right), Y_i^j\left(\overline{x}_j^{(k)}\right)\right)\right\} \end{aligned} \tag{40}$$

Considering Eq. (17), when j successively takes 1 to *m*, the maximum and minimum points set of the *i*-th output function Y_i can be obtained as follows:

$$\begin{aligned} \left(\boldsymbol{x}_i\right)_{\max} &= \left\{x_{1,\max}^{(k)}, x_{2,\max}^{(k)}, \ldots, x_{2,\max}^{(k)}\right\} \\ \left(\boldsymbol{x}_i\right)_{\min} &= \left\{x_{1,\min}^{(k)}, x_{2,\min}^{(k)}, \ldots, x_{m,\min}^{(k)}\right\} \end{aligned} \tag{41}$$

The extreme values of the *i*-th output function Y_i can be achieved at points

$(\boldsymbol{x}_i)_{\min}, (\boldsymbol{x}_i)_{\max}$.

When i successively takes the value from 1 to s, the extreme points of all elements, $\underline{Y}_j(\underline{\boldsymbol{p}}, \overline{\boldsymbol{p}}), \overline{Y}_j(\underline{\boldsymbol{p}}, \overline{\boldsymbol{p}}) (j = 1, 2, \cdots, s)$, of the output vector $\boldsymbol{Y}$ can be solved in the same way. Specifically, in step k, the structural interval outputs $\boldsymbol{Y}^I = \left[\underline{\boldsymbol{Y}}\left(\underline{\boldsymbol{p}}^{(k)}, \overline{\boldsymbol{p}}^{(k)}\right), \overline{\boldsymbol{Y}}\left(\underline{\boldsymbol{p}}^{(k)}, \overline{\boldsymbol{p}}^{(k)}\right)\right]$ with the newly updated parameter interval $\left[\underline{\boldsymbol{p}}^{(k)}, \overline{\boldsymbol{p}}^{(k)}\right]$ are obtained. Then, $\boldsymbol{Y}^I$ will be used to construct the objective function in Eq. (7). Through the outer layer bound optimization framework given in Eq. (7), the finally updated physical parameter intervals will be solved.

In the inner layer, Section 3.1 uses HDMR to represent each m-variate structural output function as the sum of m single-variate functions. Then, Section 3.2 utilizes Chebyshev polynomial approximation to calculate the stationary points of each m-variate structural output function dimension by dimension. The obtained stationary points are constants within the given optimization bounds, which helps to separate the inner and outer layers. For the outer layer bounds optimization, Section 3.3 provides an efficient stationary points updating algorithm for determining the interval structural output $\boldsymbol{Y}^I$ with the newly updated parameter interval $\left[\underline{\boldsymbol{p}}^{(k)}, \overline{\boldsymbol{p}}^{(k)}\right]$ in the optimization process. With this method, repetitive calling of the inner layer uncertainty propagation on a new interval in each optimization step is avoided.

3.4 Interval sensitivity analysis of updating parameters

Screening reasonable updating parameters is of great importance when handling complex problems. The parameters to be updated in model updating should be sensitive to structural outputs. In interval model updating, a basic interval sensitivity analysis method [50] is directly given in this section to illustrate whether the updating parameters are sensitive or not for model updating.

Local sensitivity analysis shows how the perturbation of system parameters near a given point influences the system outputs. The sensitivity of function $y = y(x_1, \ldots, x_m)$ with respect to x_i at one point $\boldsymbol{x}^0$ is defined by:

$$\frac{\partial y(\boldsymbol{x})}{\partial x_i} = \left.\frac{\partial y(x_1, \ldots, x_m)}{\partial x_i}\right|_{\boldsymbol{x}=\boldsymbol{x}^0} \tag{42}$$

In engineering problems, finite difference is an effective method to solve Eq. (42) when closed-form solution is unavailable.

$$\frac{\partial y\left(\boldsymbol{x}^{0}\right)}{\partial x_{i}}=\frac{y\left(x_{1}^{0},\ldots,x_{i}^{0}+\Delta x_{i},\ldots,x_{m}^{0}\right)-y\left(x_{1}^{0},\ldots,x_{i}^{0},\ldots,x_{m}^{0}\right)}{\Delta x_{i}} \tag{43}$$

However, traditional sensitivity analysis may lead to unreasonable results when the perturbation Δx_i is too large or too small. Hence, an interval sensitivity method is introduced to quantify the variation of the system outputs within an interval.

Consider that a component x_i^0 of $\boldsymbol{x}^0=\left(x_1^0,\ldots,x_i^0,\ldots x_m^0\right)$ is an interval variable:

$$x_{i}^{0}\in\left[\underline{x}_{i}^{0},\overline{x}_{i}^{0}\right]=\left[x_{i}^{0}-\Delta x_{i}^{0},x_{i}^{0}+\Delta x_{i}^{0}\right] \tag{44}$$

where x_i^0 and Δx_i^0 mean the interval midpoint and radius respectively.

The output $y=y\left(x_1,\ldots,x_m\right)$ at point $\boldsymbol{x}^0$ is determined by:

$$y\in y_{i}^{I}=\left[\underline{y}_{i}^{0},\overline{y}_{i}^{0}\right]=y\left(x_{1}^{0},\ldots,\left[x_{i}^{0}-\Delta x_{i},x_{i}^{0}+\Delta x_{i}\right],\ldots,x_{m}^{0}\right) \tag{45}$$

The variation of the output y can be described by the interval radius Δy_i^0 of y^I :

$$\Delta y_{i}^{0}=\frac{\overline{y}_{i}^{0}-\underline{y}_{i}^{0}}{2} \tag{46}$$

Then, its relative sensitivity at point $\boldsymbol{x}^0$ is defined by:

$$\frac{\Delta y_{i}^{0}}{\Delta x_{i}^{0}}=\frac{\overline{y}_{i}^{0}-\underline{y}_{i}^{0}}{\overline{x}_{i}^{0}-\underline{x}_{i}^{0}} \tag{47}$$

This index reflects the change of the output y regarding x_i within interval $\left[\underline{x}_i^0,\overline{x}_i^0\right]$ and helps to determine whether the parameters to be updated are feasible.

4 Flowchart of the Algorithmic Implementation

In this study, an interval model updating method based on HDMR and polynomials approximation is proposed when insufficient information of uncertain variables is provided. Firstly, each multivariate structural output function is decomposed into multiple single-variate functions. Their stationary points are estimated using polynomials approximation on initial interval $[\boldsymbol{UB},\boldsymbol{LB}]$. Then, the interval parameters are updated under the optimization framework. The implementation of the proposed methodology is summarized in Table 1. For clarity, the flowchart of the proposed method is given in Figure 4 to further illustrate the proposed method.

Table 1: Algorithmic implementation of the proposed interval model updating method

	Implementation: interval model updating
1.	specify the upper and lower bounds of the parameters to be updated: $\boldsymbol{UB}, \boldsymbol{LB}$
2.	**for** $i = 1, 2, \cdots, s$ **do**
3.	determine the object: the ***i***-th structural output Y_i
4.	construct the reduced-order representation model of Y_i through Eq. (17) at the midpoint $\boldsymbol{p}^c$ of the interval variable $\boldsymbol{p}$
5.	**for** $j = 1, 2, \cdots, m$ **do**
6.	construct the approximation $H_r\left(x_j\right)$ of $Y_i^j\left(p_j\right) \doteq Y_i^j\left(x_j\right)$ through Eq. (22) – Eq. (28) on interval $p_j \in \left[LB_j, UB_j\right]$
7.	solve the stationary points $\left\{x_{j,d}\right\}$ of $Y_i^j\left(p_j\right) \doteq Y_i^j\left(x_j\right)$ through Eq. (29) - Eq. (31)
8.	**end for**
9.	**end for**
10.	given the upper and lower bounds of the optimization parameters: $\boldsymbol{UB}, \boldsymbol{LB}$; the upper and lower bounds $\overline{\boldsymbol{Y}}^e, \underline{\boldsymbol{Y}}^e$ of the test outputs used in Eq. (7)
11.	initialize the interval bounds of the parameters: $\underline{\boldsymbol{p}}, \overline{\boldsymbol{p}}$
12.	**for** $i = 1, 2, \cdots, s$ **do**
13.	obtain the reference stationary points $\left\{x_{j,d}\right\}^{(ref)}$ by Eq. (34) – Eq. (35) based on the stationary points calculated in 7.
14.	in each optimization step, new stationary points are obtained using Eq. (36) - Eq. (39)
15.	solve the extreme points of output Y_i through Eq. (40) - Eq. (41) , and then solve the interval bounds $\overline{Y}_i, \underline{Y}_i$ of Y_i
16.	**end for**
17.	calculate the fitness function (objective function) in Eq. (7)
18.	update the interval parameters $\underline{\boldsymbol{p}}, \overline{\boldsymbol{p}}$ through the optimization strategy
19.	repeat step 12 – step 16 until termination conditions are satisfied

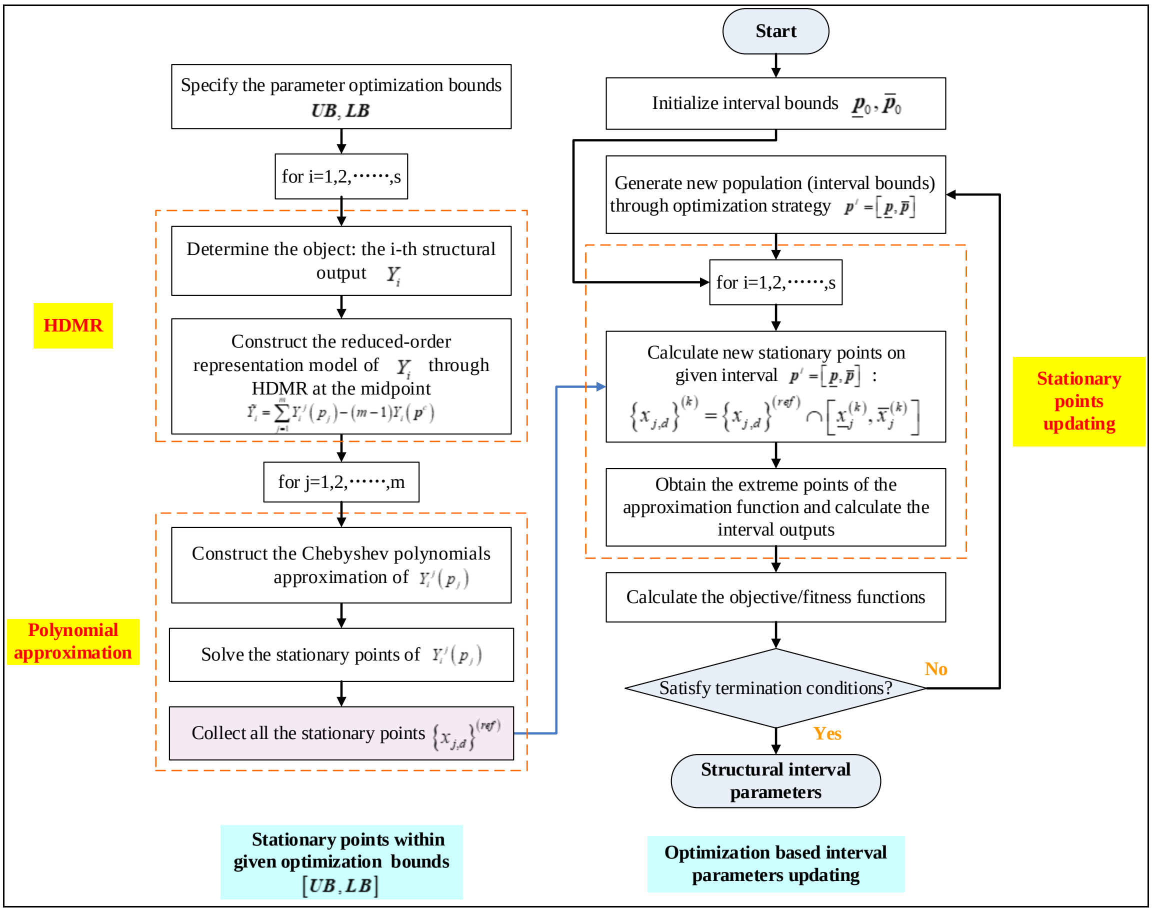

Figure 4: The flowchart of the proposed interval model updating method

5 Case Studies

In this section, two numerical examples and one experimental example are utilized to verify the effectiveness and accuracy of the proposed interval model updating scheme.

5.1 *Numerical case studies*

5.1.1 Case 1: numerical validation of a spring-mass system

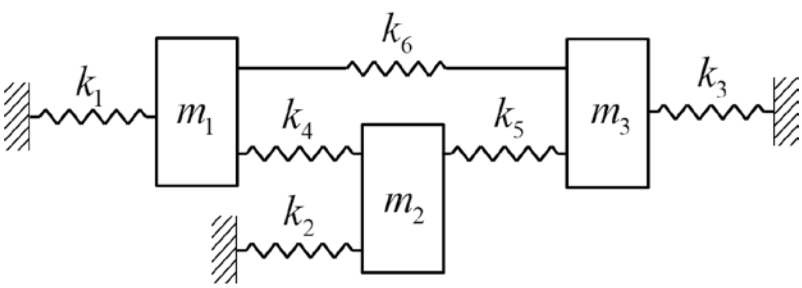

Figure 5: The spring-mass system

This case is a spring-mass system with three degree-of-freedoms (DOFs) from [26] and it is shown in Figure 5. For comparison purpose, the first three eigenvalues $\lambda_1, \lambda_2, \lambda_3$ of the structure system and the absolute value of the first component of the first order mode shape $\left|\phi(1,1)\right|$ are taken as the structural interval outputs. Two scenarios (update stiffness parameters and update stiffness and mass parameters) are considered.

5.1.1.1 Update stiffness parameters

The true parameters of the spring-mass system are given as follows:

$$m_1 = m_2 = m_3 = 1 \text{ (kg)};\ k_3 = k_4 = 1, k_6 = 3 \text{ (N/m)};\ k_1 = k_2 = k_5 = [0.8, 1.2] \text{ (N/m)}.$$

The stiffness of three springs k_1, k_2, k_5 are selected as interval parameters to be updated. Their initial intervals are $k_1 = k_2 = k_5 = [0.5, 1.5]$ (N/m). Table 2 shows the interval sensitivity of the outputs with respect to the interval parameters. It is clear that there are at least two parameters among k_1, k_2, k_5 influencing the structural outputs. Hence, the chosen parameters are feasible for model updating.

Table 2: Interval sensitivity of the outputs with respect to the updating parameters (k_1, k_2, k_5)

Sensitivity	λ_1	λ_2	λ_3	$\left\|\phi(1,1)\right\|$
k_1	0.3339	0.1662	0.4999	0.0731
k_2	0.3354	0.6646	0.0000	0.0641
k_5	0.0000	1.4885	0.5115	0.0000

The updated parameters intervals using proposed method are given in Table 3. Error* means the updating errors in [26]. After model updating using the proposed method, the interval bounds of k_1, k_2, k_5 coincide well with the true intervals. The mean error of the interval bounds decreases from $[-37.5, 25.0]$% to $[0.16, 0.54]$%. Compared with [26] of which the mean error is $[0.4, 0.3]$%, the proposed method has better updating performance. Figure 6 shows the initial, true and updated output spaces of the spring-mass system. It is clear that the true and updated output spaces coincide with each other well.

Table 3: Updated interval bounds of the spring-mass system (k_1, k_2, k_5)

Parameter	True	Initial	Error (%)	Updated	Error (%)	Error*(%)
k_1	$[0.8, 1.2]$	$[0.5, 1.5]$	$[-37.5, 25.0]$	$[0.80, 1.21]$	$[0.14, 0.73]$	$[1.3, 0]$
k_2	$[0.8, 1.2]$	$[0.5, 1.5]$	$[-37.5, 25.0]$	$[0.80, 1.19]$	$[-0.30, -0.68]$	$[0, 0.8]$

k_5	$[0.8,1.2]$	$[0.5,1.5]$	$[-37.5,25.0]$	$[0.80,1.20]$	$[0.09,0.23]$	$[0,0]$
mean			$[-37.5,25.0]$		$[0.16,0.54]$	$[0.4,0.3]$

Note: The data of Error* are taken from [26] for comparison.

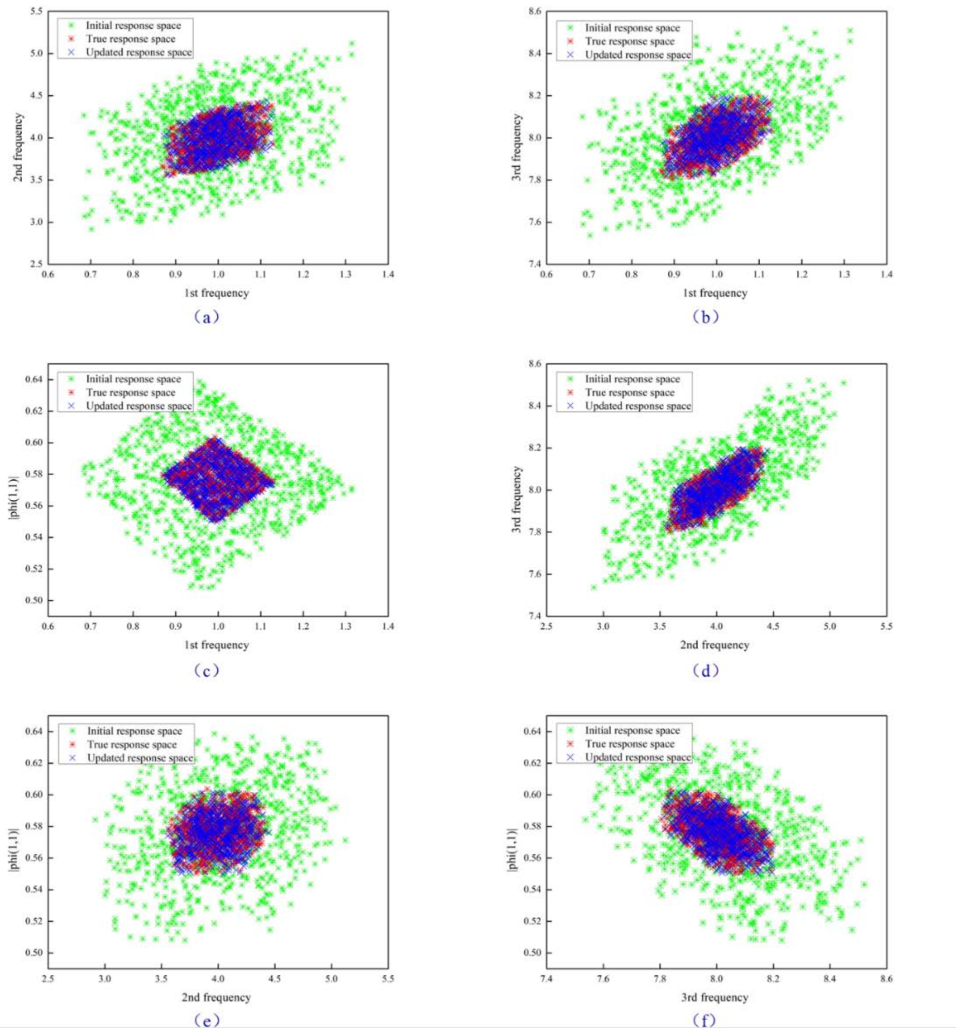

Figure 6: Initial, true and updated output spaces of the spring-mass system (k_1, k_2, k_5): (a) output space of the 1st and 2nd frequencies; (b) output space of the 1st and 3rd frequencies; (c) output space of the 1st frequency and the first absolute component of the 1st mode shape; (d) output space of the 2nd and 3rd frequencies; (e) output space of the 2nd frequency and the first absolute component of the 1st mode shape; (f) output space of the 3rd frequency and the first absolute component of the 1st mode shape

5.1.1.2 Update stiffness and mass parameters simultaneously

Suppose the actual parameters of the spring-mass system are given as follows:

$m_1 = m_2 = 1, m_3 = [0.8,1.2]$ (kg); $k_3 = k_4 = k_5 = 1, k_6 = 3$ (N/m); $k_1 = k_2 = [0.8,1.2]$ (N/m).

The stiffness of two springs k_1, k_2 and mass m_3 are chosen as interval parameters to be updated. Their initial intervals are $k_1 = k_2 = [0.5, 1.5]$ (N/m), $m_3 = [0.5, 1.5]$ (kg). The interval sensitivity results of the outputs with respect to the interval parameters are given in Table 4. λ_3 is sensitive to k_1 and m_3, while the remaining three model outputs are sensitive to all parameters. As a result, the parameters to be updated include k_1, k_2 and m_3.

Table 4: Interval sensitivity of the model outputs with respect to the updating parameters (k_1, k_2, m_3)

Sensitivity	λ_1	λ_2	λ_3	$\lvert\phi(1,1)\rvert$
k_1	0.3339	0.1662	0.4999	0.0731
k_2	0.3354	0.6646	0.0000	0.0641
m_3	0.3324	0.6386	5.6957	0.1017

Table 5: Updated interval bounds of the spring-mass system (k_1, k_2, m_3)

Parameter	True	Initial	Error (%)	Updated	Error (%)	Error*(%)
k_1	$[0.8, 1.2]$	$[0.5, 1.5]$	$[-37.5, 25.0]$	$[0.80, 1.20]$	$[0.03, -0.03]$	$[2.5, -1.7]$
k_2	$[0.8, 1.2]$	$[0.5, 1.5]$	$[-37.5, 25.0]$	$[0.80, 1.20]$	$[-0.02, 0.03]$	$[0, 2.5]$
m_3	$[0.8, 1.2]$	$[0.5, 1.5]$	$[-37.5, 25.0]$	$[0.80, 1.20]$	$[0.00, 0.01]$	$[2.5, 0]$
mean			$[-37.5, 25.0]$		$[0.02, 0.02]$	$[1.7, 1.4]$

Note: The data of Error* are taken from [26] for comparison.

The updated parameters intervals using proposed method are given in Table 5. After updating, the interval bounds of k_1, k_2, m_3 coincide well with the true intervals. The mean error of the interval bounds decreases from $[-37.5, 25.0]$% to $[0.02, 0.02]$%. Compared with [26] whose mean error was given as $[1.7, 1.4]$ %, the proposed method has a better performance. Figure 7 shows the initial, true and updated output spaces of the spring-mass system. Compared with initial output space, the updated one is narrower, which indicates that the true and updated output spaces coincide with each other well.

In order to further show the efficiency of the proposed method. Case 1 is computed using both the proposed method and the approach in [29] on MATLAB R2018b platform, and the mean computation time of 5 runs for interval bounds optimization is given in Table 6.

It is obvious that the proposed method spends less time to optimize the parameter bounds for different updating parameters.

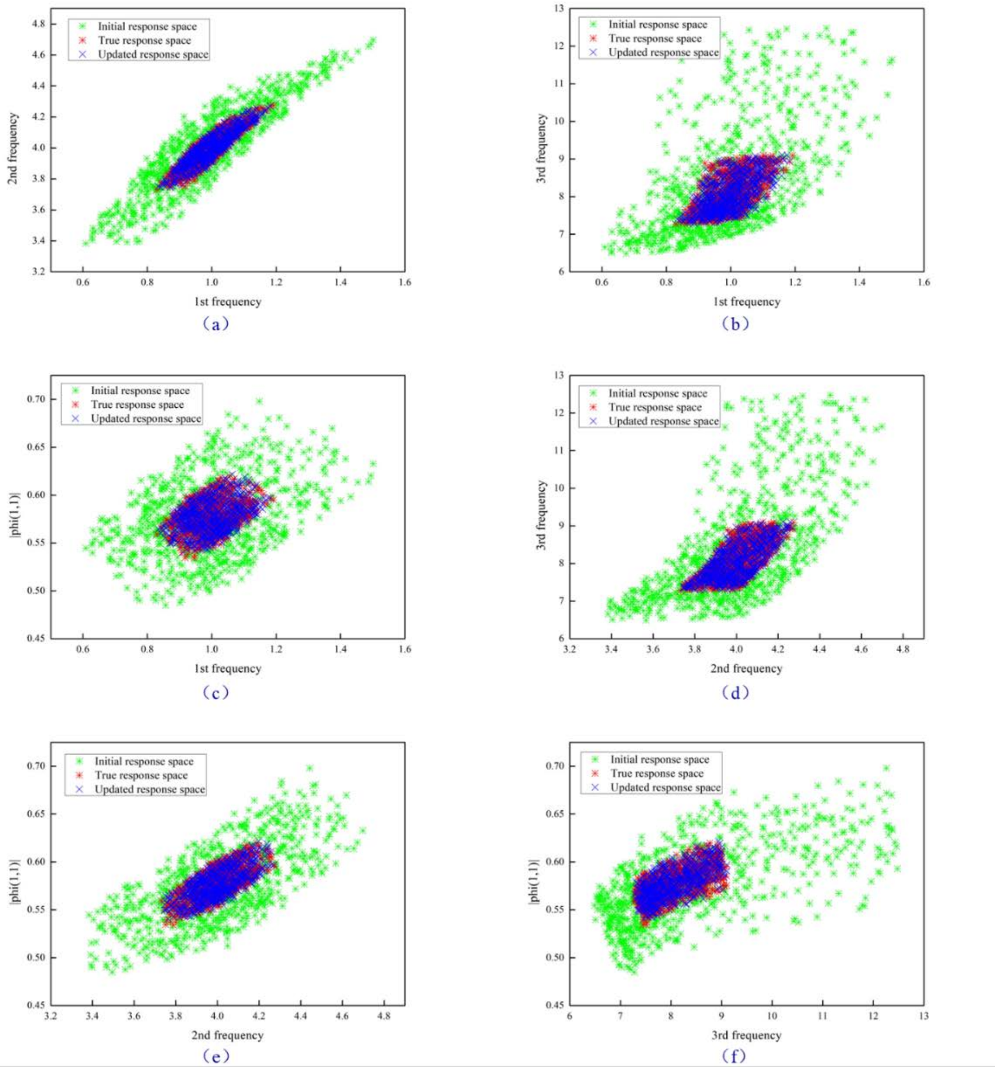

Figure 7: Initial, true and updated output spaces of the spring-mass system (k_1, k_2, m_3): (a) output space of the 1st and 2nd frequencies; (b) output space of the 1st and 3rd frequencies; (c) output space of the 1st frequency and the first absolute component of the 1st mode shape; (d) output space of the 2nd and 3rd frequencies; (e) output space of the 2nd frequency and the first absolute component of the 1st mode shape; (f) output space of the 3rd frequency and the first absolute component of the 1st mode shape

Table 6: Optimization time of the proposed method and method in [29]

	Proposed method		Method in [29]	
Updating parameters	k_1, k_2, k_5	k_1, k_2, m_3	k_1, k_2, k_5	k_1, k_2, m_3

Optimization Time (s)	74.91	143.13	147.88	197.91

5.1.2 Case 2: numerical validation of Canton Tower

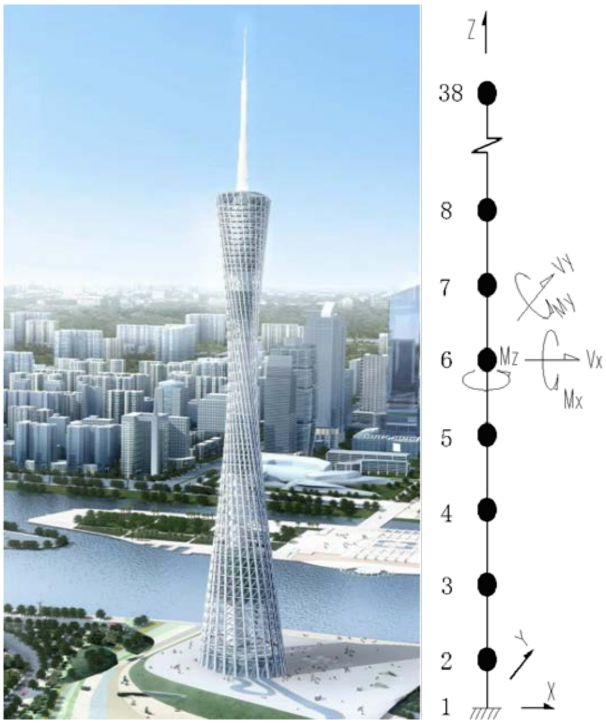

Figure 8: Real and numerical models of the Canton Tower [51]

The Canton Tower (Guangzhou TV Tower) is located in Guangdong Province, China. It consists of a main tower with a height of 454m and an antenna mast with a height of 146m, with a total height of 600m and 37 floors above the ground. The tower is composed of a reinforced concrete inner core tube, a steel outer frame tube and a combined floor connecting the two. Current research has established the full FE model and reduced FE model of the Canton Tower. In [52-54], the entire structure is divided into 37 segments, each of which is modeled as a linear elastic beam element. As shown in Figure 8, the reduced FE model consists of 37 beam elements and 38 nodes. The main tower consists of 27 elements and the mast is modeled as 10 elements. In the reduced FE model, the vertical displacement of each node is disregarded, and hence each node has 5 DOFs (two horizontal translational DOFs and three rotational DOFs). The first node is completely fixed to the ground and the entire model has 185 DOFs in total.

Considering that the elastic and shear modulus coefficients X_k, X_g of the FE model are the most important parameters in the model simplification, these two quantities are used as interval variables to be updated in this case. Following [54], the experimental mode information of the Canton Tower is obtained based on the global FE model of the tower. In this case, the first four natural frequencies (Hz) are used as the structural interval outputs for model updating. The interval sensitivity results of these four natural frequencies with respect to the elastic and shear modulus coefficients are listed in Table 7. The results illustrate that both parameters will influence the natural frequencies, which is reasonable. Furthermore, it is clear that the natural frequencies are much more sensitive to the shear modulus coefficient in this model. Hence, the updating intervals of the shear modulus coefficient are narrower than that of the elastic modulus coefficient.

Table 7: Interval sensitivity of the outputs with respect to the updating parameters (X_k, X_g)

Sensitivity	λ_1	λ_2	λ_3	λ_4
X_k	0.0592	0.0851	0.1856	0.1977
X_g	1.9807	1.7357	7.0938	9.8480

Table 8: Updated interval bounds of the Canton Tower (X_k, X_g)

Parameter	True	Initial	Error (%)	Updated	Error (%)
X_k	$[0.85, 0.90]$	$[0.75, 1.00]$	$[-11.8, 11.1]$	$[0.851, 0.903]$	$[0.14, 0.73]$
X_g	$[0.995, 1.005]$	$[0.99, 1.01]$	$[-0.5, 0.5]$	$[0.995, 1.005]$	$[0, 0]$
mean			$[6.15, 5.8]$		$[0.07, 0.37]$

Table 9: The first four frequencies of the Canton Tower under true, initial and updated states

Frequency	True(Hz)	Initial(Hz)	Error (%)	Updated(Hz)	Error (%)
f_1	$[0.0917, 0.1137]$	$[0.0746, 0.1279]$	$[-18.68, 12.44]$	$[0.0919, 0.1136]$	$[0.27, -0.11]$
f_2	$[0.1376, 0.1586]$	$[0.1196, 0.1745]$	$[-13.10, 10.02]$	$[0.1378, 0.1586]$	$[0.16, -0.02]$
f_3	$[0.2811, 0.3491]$	$[0.2007, 0.3818]$	$[-28.59, 9.37]$	$[0.2818, 0.3491]$	$[0.27, -0.01]$
f_4	$[0.2876, 0.3910]$	$[0.2025, 0.4423]$	$[-29.59, 13.13]$	$[0.2884, 0.3903]$	$[0.27, -0.17]$
mean			$[22.49, 11.24]$		$[0.25, 0.08]$

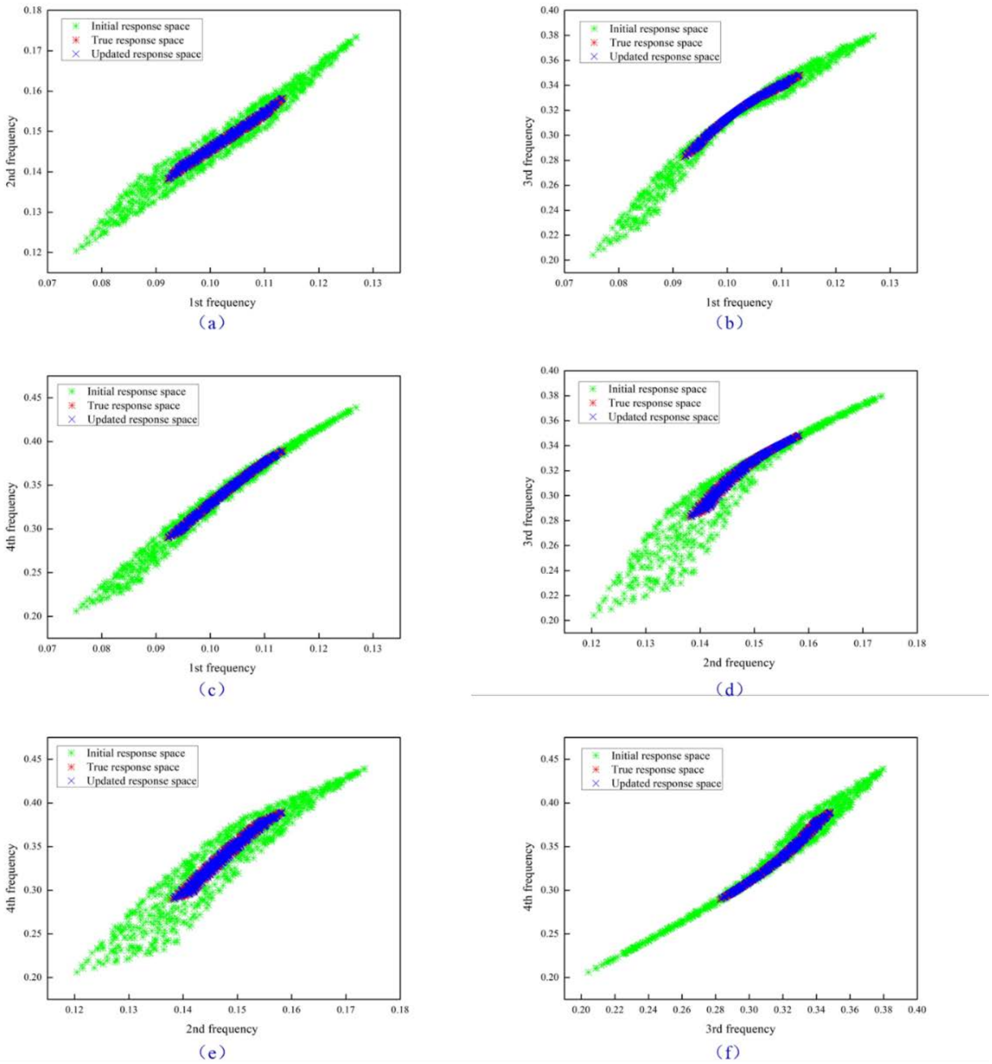

Figure 9: Initial, true and updated output spaces of the Canton Tower: (a) output space of the 1st and 2nd frequencies; (b) output space of the 1st and 3rd frequencies; (c) output space of the 1st and 4th frequencies; (d) output space of the 2nd and 3rd frequencies; (e) output space of the 2nd and 4th frequencies; (f) output space of the 3rd and 4th frequencies

From Table 8, the updated elastic and shear modulus coefficients X_k, X_g of the FE model have a good match with their true values. The maximum updating error is small. It should be noted that the structure is very sensitive to the shear modulus coefficient X_g, thus its variation interval is narrow.

The true, initial and updated output spaces of the Canton Tower are shown in Figure 9 and the first four natural frequencies of the Canton Tower before and after updating are given in Table 9. According to Figure 9, the true, initial and updated output spaces of the Canton

Tower are coincident, which also illustrates the effectiveness of the proposed updating method. From Table 9, it is obvious that the structural natural frequencies based on the updated structural parameters are consistent with the true ones. Although the frequencies in this case are small and the third and fourth frequencies are very close, the proposed method can still update the structural parameters with satisfactory results.

5.2 Experimental case studies

5.2.1 Case 1: experimental verification of a free-free plate

In this experimental verification, a series of nominally identical steel plates (600mm × 120 mm × 3mm) [26] are considered. In the original literature, 55 nominally identical steel plates were tested in the laboratory with a free–free boundary condition as shown in Figure 10. The geometrical parameters for all these plates theoretically are 600mm(length) × 120 mm(width) × 3mm(thickness). The finite element model of these plates can be constructed as Figure 11 which comprises of 300 equal size elements. In this case, the first five natural frequencies of these plates were regarded as the structural uncertain outputs used for interval model updating. The real natural frequencies of these plates were obtained through modal tests in the laboratory.

Figure 10: The steel plate with free-free boundaries in laboratory [26]

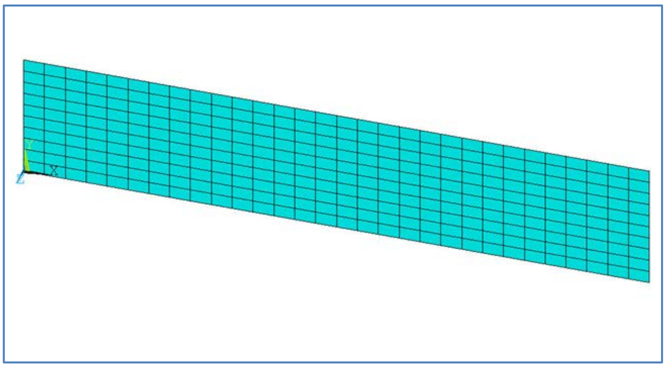

Figure 11: The finite element model of the steel plate

After testing, the true/measured intervals of the first five natural frequencies are obtained by interval uncertainty quantification as follows:

$$f_i \in f_i^I = \left[\underline{f}_i, \overline{f}_i \right] \left(i = 1, 2, \cdots, 5 \right) \tag{48}$$

$$\begin{aligned} \underline{f}_i &= \min_{j=1,\cdots,55} \left(f_i^j \right) \\ \overline{f}_i &= \max_{j=1,\cdots,55} \left(f_i^j \right) \end{aligned} \tag{49}$$

where f_i means the *i*-th natural frequency, $\underline{f}_i, \overline{f}_i$ are its interval bounds, and f_i^j denotes the *i*-th natural frequency of the *j*-th plate.

In this model updating verification, the parameters to be updated are the elastic and shear modulus E, G of the steel plate. According to several single axis tension tests, the initial intervals of E, G are set as $E = [190, 220]$ GPa and $G = [77, 89]$ GPa. Table 10 shows the interval sensitivity of the outputs with respect to the interval parameters. The five frequencies vary significantly the elastic and shear modulus change.

Table 10: Interval sensitivity of the outputs with respect to the updating parameters (E, G)

Sensitivity	f_1	f_2	f_3	f_4	f_5
E	0.1105	0.3303	0.0113	0.7082	0.0899
G	0.0088	0.0844	0.7945	0.3032	1.4584

The updating results are given in Table 11. In order to verify the performance of the model updating, the interval bounds of the first five natural frequencies under measured, initial and updated states are given in Table 12. After updating, the interval bounds of the outputs coincide well with the measured intervals. The mean error of the interval bounds decreases from $[1.79,4.03]$% to $[0.31,0.16]$%. Compared with [26] of which the mean error is $[0.4,0.2]$%, the proposed method has a better updating effect. It is clear that the practical output intervals are relatively narrow since a small variation in structural stiffness coefficient usually leads to a small variation in natural frequencies. Results in Table 12 show that the predicted interval frequencies of higher orders have larger errors than frequencies of lower orders.

Table 11: Updated interval bounds of the steel plate (E,G)

Parameter	Initial	Updated	Updated*
E (GPa)	$[190,220]$	$[195.9,203.3]$	$[196.5,203.6]$
G (GPa)	$[77,89]$	$[79.1,83.1]$	$[79.5,83.4]$

Note: The data of Error* are taken from [26] for comparison.

Table 12: Outputs interval bounds of the steel plate under measured, initial and updated states

Frequency	Measured(Hz)	Initial(Hz)	Error (%)	Updated(Hz)	Error (%)	Updated* (Hz)	Error*(%)
f_1	$[42.66,43.64]$	$[42.12,45.50]$	$[1.27,4.26]$	$[42.81,43.67]$	$[0.36,0.07]$	$[42.87,43.71]$	$[0.5,0.2]$
f_2	$[118.29,121.03]$	$[116.16,126.62]$	$[1.80,4.62]$	$[118.31,121.02]$	$[0.02,-0.01]$	$[118.45,121.11]$	$[0.1,0.1]$
f_3	$[133.24,136.54]$	$[131.48,141.32]$	$[1.32,3.50]$	$[133.24,136.54]$	$[0.00,0.00]$	$[133.58,136.79]$	$[0.3,0.2]$
f_4	$[234.07,239.20]$	$[227.77,250.55]$	$[2.69,4.74]$	$[232.56,238.60]$	$[-0.6,-0.25]$	$[232.78,238.78]$	$[-0.6,-0.2]$
f_5	$[274.29,280.64]$	$[269.10,289.20]$	$[1.89,3.05]$	$[272.80,279.38]$	$[-0.5,-0.45]$	$[273.45,279.86]$	$[-0.3,-0.3]$
mean			$[1.79,4.03]$		$[0.31,0.16]$		$[0.4,0.2]$

Note: The data of Measured, Initial, Updated* and Error* are taken from [26] for comparison.

5.2.2 Case 2: experimental verification of Canton Tower

The structural model information of the Canton Tower is given in 5.1.2 Case 2. This section will introduce the experimental aspect of the tower. According to [51], the tower was equipped with a structural health monitoring system in which twenty uni-axial accelerometers (Tokyo Sokushin AS-2000C) were employed for vibration measurement. The accelerometers have a frequency range of DC-50 Hz (3 dB), an amplitude range of ±2 g and a sensitivity of 1.25 V/g. Structural acceleration data from 18:00 pm 19th Jan. 2010 to 18:00 pm 20th Jan. 2010 (in total 24 hours) were recorded with the sampling frequency of 50Hz by the monitoring system.

In this case, the collected acceleration series were split into nonoverlapping 20-min segments, and each segment was used for natural frequency extraction. Through operational modal analysis, the natural frequencies of all the 72 segments are extracted. Structural responses from repeated experiments will contain variations due to environment noise, numerical error, etc. [55]. Similar to Eq. (48) and Eq. (49), the measured intervals of the first four natural frequencies are obtained by interval uncertainty quantification. The measured interval natural frequencies are given in Table 14.

This experimental verification mainly considers the variability of the structural natural frequencies, and the uncertainties are reflected by both the interval descriptions of the measured frequencies and the structural physical parameters to be updated. An initial Ansys model was firstly constructed, and then it was simplified as a reduced order FE model [51]. The fine-tuned FE model is employed for model updating. Similar to 5.1.2 Case 2, the elastic and shear modulus coefficients X_k, X_g of the FE model are chosen as interval variables to be updated herein. The interval sensitivities of the structural natural frequencies with respect to the chosen two structural parameters have been analyzed and given in Table 7. It is obvious that the four natural frequencies are sensitive to the selected structural parameters.

Table 13: Updated interval bounds of the Canton Tower (X_k, X_g)

Parameter	Initial	Updated
X_k	$[0.97, 1.03]$	$[0.9898, 1.0102]$
X_g	$[0.99, 1.01]$	$[0.9999, 1.0001]$

Table 14: Outputs interval bounds of the Canton Tower under measured and updated states

Frequency	Measured(Hz)	Updated(Hz)	Error (%)
f_1	$[0.0925, 0.0943]$	$[0.0925, 0.0943]$	$[0.00, -0.01]$
f_2	$[0.1372, 0.1392]$	$[0.1373, 0.1390]$	$[0.10, -0.11]$
f_3	$[0.3640, 0.3681]$	$[0.3640, 0.3681]$	$[0.00, 0.00]$
f_4	$[0.4227, 0.4249]$	$[0.4213, 0.4262]$	$[-0.32, 0.32]$
mean			$[0.11, 0.11]$

The updating results are given in Table 13. The updated structural parameters intervals are much narrower than their initial counterparts. The interval width of the shear modulus coefficient is very small compared with that of the elastic modulus coefficient since the structural outputs are much more sensitive to the shear modulus coefficient. The interval bounds of the first four natural frequencies under measured and updated states are given in

Table 14. After updating, the mean error (absolute value) of the interval bounds reaches a low level of $[0.11, 0.11]\%$. The measured, initial, and updated output spaces of the Canton Tower are shown in Figure 12. Compared with the initial output space, the updated output space has a good agreement with the measured output space. From both Table 14 and Figure 12, the upper and lower bounds of the updated output space are close to corresponding bounds of the measured output space, which shows the effectiveness of the proposed interval model updating method.

Through the above cases, the effectiveness of the proposed method is well illustrated. Compared with the interval response surface method in [26], the proposed method obtain better updating results. In some cases, the interval response surface model is unable to represent the structural input-output relation and Box-Cox transformation is needed. The approach in [29] updates interval midpoint and radius respectively. It employs Monte Carlo method to propagate uncertainties forward with a high precision but relatively low efficiency compared with the proposed method. The proposed method makes full use of HDMR and Chebyshev polynomials to decouple the inner and outer layers of interval model updating, and utilizes the stationary points updating strategy to optimize parameter bounds efficiently. Hence, it achieves a good trade-off between efficiency and accuracy.

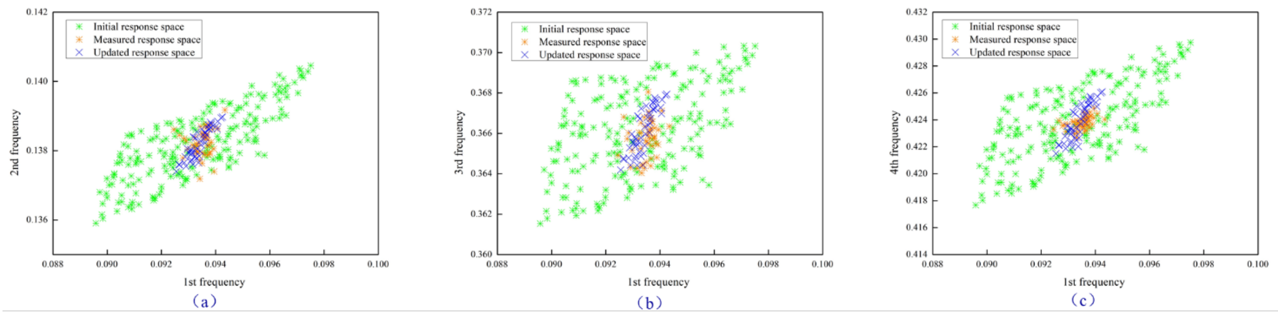

Figure 12: Initial, measured and updated output spaces of the Canton Tower: (a) output space of the 1st and 2nd frequencies; (b) output space of the 1st and 3rd frequencies; (c) output space of the 1st and 4th frequencies

5 Conclusions

While interval uncertainty is promising for identifying uncertain-but-bounded physical parameters, interval model updating is still challenging due to complex models and huge computational burden involved in the repeated evaluation of non-probabilistic constraints. This paper proposes a new scheme to improve the performance of existing interval model updating algorithms based on new algorithms. The first algorithm is characterized by a decoupling strategy to realize the independent operation of inner uncertainty propagation and outer interval optimization originally interacted with each other through decomposing the model input-output functions into the sum of multiple single-variate functions using HDMR, while each single-variate function is further approximated by Chebyshev polynomial approximation. The second algorithm aims to enhance the search efficiency of the bounds through an efficient optimization strategy with the aid of stationary points of Chebyshev polynomials so as to avoid brute-force and time-consuming interval optimization. Based on the proposed method, two numerical examples and two experimental applications show their capabilities of updating structural parameters with interval uncertainty. The updated results (interval upper and lower bounds) and outputs spaces matched well with corresponding true values. Furthermore, these results show that the proposed scheme outperforms a classic interval response surface method. However, some improvements are still needed in further study. Although the HDMR technique shows its effectiveness here, the discrepancy of the first-order HDMR will increase with the increase of model complexity, and higher-order HDMR including cross-terms ought to be utilized. Hence, the trade-off between computation efficiency and computation accuracy for more complex problems is still a critical issue worth of further investigation in the future.

Acknowledgements

Financial support to complete this study was provided by the Science and Technology Development Fund, Macau SAR (File no.: FDCT/017/2020/A1, FDCT/0101/2021/A2, FDCT/0010/2021/AGJ and SKL-IOTSC(UM)-2021-2023), the Research Committee of University of Macau (File no.: MYRG2020-00073-IOTSC, MYRG2022-00096-IOTSC and SRG2019-00194-IOTSC) and Guangdong-Hong Kong-Macau Joint Laboratory Program (Project No.: 2020B1212030009). The views and opinions expressed in this article are those of the authors and do not necessarily reflect those of the sponsors.

References

[1] M. Friswell, J.E. Mottershead, Finite element model updating in structural dynamics,

Springer Science & Business Media, 1995.

[2] K.-V. Yuen, Bayesian methods for structural dynamics and civil engineering, John Wiley & Sons, 2010.

[3] W.-J. Yan, S.-Z. Cao, W.-X. Ren, K.-V. Yuen, D. Li, L. Katafygiotis, Vectorization and distributed parallelization of Bayesian model updating based on a multivariate complex-valued probabilistic model of frequency response functions, Mechanical Systems and Signal Processing, 156 (2021) 107615.

[4] M. Kitahara, S. Bi, M. Broggi, M. Beer, Nonparametric Bayesian stochastic model updating with hybrid uncertainties, Mechanical Systems and Signal Processing, 163 (2022) 108195.

[5] S. Sehgal, H. Kumar, Structural Dynamic Model Updating Techniques: A State of the Art Review, Archives of Computational Methods in Engineering, 23 (2016) 515-533.

[6] J.E. Mottershead, M. Friswell, Model updating in structural dynamics: a survey, Journal of sound and vibration, 167 (1993) 347-375.

[7] E. Simoen, G. De Roeck, G. Lombaert, Dealing with uncertainty in model updating for damage assessment: A review, Mechanical Systems and Signal Processing, 56-57 (2015) 123-149.

[8] S.E. Fang, Q.H. Zhang, W.X. Ren, Parameter variability estimation using stochastic response surface model updating. Mechanical Systems and Signal Processing, 49(1-2), (2014) 249-263.

[9] K. Jurado, S.C. Ludvigson, S. Ng, Measuring uncertainty, American Economic Review, 105 (2015) 1177-1216.

[10] M. Chandrashekhar, R. Ganguli, Damage assessment of composite plate structures with material and measurement uncertainty, Mechanical Systems and Signal Processing, 75 (2016) 75-93.

[11] C. Soize, Uncertainty Quantification, Springer, 2017.

[12] Z.P. Qiu, L. Wang, The need for introduction of non-probabilistic interval conceptions into structural analysis and design, Science China-Physics Mechanics & Astronomy, 59 (2016).

[13] N.A.Z. Abdullah, M.S.M. Sani, M.M. Rahman, I. Zaman, Iop, A review on model updating in structural dynamics, 3rd International Conference on Mechanical Engineering Research (ICMER), Kuantan, MALAYSIA, 2015.

[14] X. Jia, O. Sedehi, C. Papadimitriou, L.S. Katafygiotis, B. Moaveni, Hierarchical

Bayesian modeling framework for model updating and robust predictions in structural dynamics using modal features. Mechanical Systems and Signal Processing, 170 (2022) 108784.

[15] C. Mares, J.E. Mottershead, M.I. Friswell, Stochastic model updating: Part 1 - theory and simulated example, Mechanical Systems and Signal Processing, 20 (2006) 1674-1695.

[16] J. Mo, L. Wang, Z. Qiu, Q. Shi, A nonprobabilistic structural damage identification approach based on orthogonal polynomial expansion and interval mathematics. Structural Control and Health Monitoring, 26(8) (2019) e2378.

[17] G. Alefeld, G. Mayer, Interval analysis: theory and applications, Journal of computational and applied mathematics, 121 (2000) 421-464.

[18] Y. Ben-Haim, I. Elishakoff, Convex models of uncertainty in applied mechanics, Elsevier, 2013.

[19] D. Moens, D. Vandepitte, A survey of non-probabilistic uncertainty treatment in finite element analysis, Computer methods in applied mechanics and engineering, 194 (2005) 1527-1555.

[20] J. Zheng, Z. Luo, C. Jiang, J. Gao, Robust topology optimization for concurrent design of dynamic structures under hybrid uncertainties, Mechanical Systems and Signal Processing, 120 (2019) 540-559.

[21] M. Faes, D. Moens, Recent trends in the modeling and quantification of non-probabilistic uncertainty, Archives of Computational Methods in Engineering, 27 (2020) 633-671.

[22] J. Mo, L. Wang, K. Gu, A two-step interval structural damage identification approach based on model updating and set-membership technique, Measurement, 182 (2021) 109464.

[23] M.-Y. Zhao, W.-J. Yan, K.-V. Yuen, M. Beer, Non-probabilistic uncertainty quantification for dynamic characterization functions using complex ratio interval arithmetic operation of multidimensional parallelepiped model, Mechanical Systems and Signal Processing, 156 (2021) 107559.

[24] H.H. Khodaparast, J. Mottershead, K. Badcock, Interval model updating: method and application, Proc. of the ISMA, University of Leuven, Belgium, (2010).

[25] H.H. Khodaparast, J.E. Mottershead, K.J. Badcock, Interval model updating with irreducible uncertainty using the Kriging predictor, Mechanical Systems and Signal

Processing, 25 (2011) 1204-1226.

[26] S.-E. Fang, Q.-H. Zhang, W.-X. Ren, An interval model updating strategy using interval response surface models, Mechanical Systems and Signal Processing, 60-61 (2015) 909-927.

[27] Z. Deng, Z. Guo, X. Zhang, Interval model updating using perturbation method and Radial Basis Function neural networks, Mechanical Systems and Signal Processing, 84 (2017) 699-716.

[28] B. Zheng, K. Yu, S. Liu, R. Zhao, Interval model updating using universal grey mathematics and Gaussian process regression model, Mechanical Systems and Signal Processing, 141 (2020) 106455.

[29] Z. Deng, Z. Guo, Interval identification of structural parameters using interval overlap ratio and Monte Carlo simulation, Advances in Engineering Software, 121 (2018) 120-130.

[30] Y. Zhao, J. Yang, M.G. Faes, S. Bi, Y. Wang, The sub-interval similarity: A general uncertainty quantification metric for both stochastic and interval model updating, Mechanical Systems and Signal Processing, 178 (2022) 109319.

[31]M.G. Faes, M.A. Valdebenito, Fully decoupled reliability-based design optimization of structural systems subject to uncertain loads, Computer Methods in Applied Mechanics and Engineering, 371 (2020) 113313.

[32] M.G. Faes, M.A. Valdebenito, D. Moens, M. Beer, Bounding the first excursion probability of linear structures subjected to imprecise stochastic loading, Computers & Structures, 239 (2020) 106320.

[33] M.G. Faes, M.A. Valdebenito, D. Moens, M. Beer, Operator norm theory as an efficient tool to propagate hybrid uncertainties and calculate imprecise probabilities, Mechanical Systems and Signal Processing, 152 (2021) 107482.

[34] X.-X. Liu, I. Elishakoff, A combined Importance Sampling and active learning Kriging reliability method for small failure probability with random and correlated interval variables, Structural safety, 82 (2020) 101875.

[35] H. Ouyang, J. Liu, X. Han, G. Liu, B. Ni, D. Zhang, Correlation propagation for uncertainty analysis of structures based on a non-probabilistic ellipsoidal model, Applied Mathematical Modelling, 88 (2020) 190-207.

[36] B. Liao, R. Zhao, K. Yu, C. Liu, A novel interval model updating framework based on correlation propagation and matrix-similarity method, Mechanical Systems and Signal

Processing, 162 (2022) 108039.

[37] H. Ouyang, J. Liu, X. Han, B. Ni, G. Liu, Y. Lin, Non-probabilistic uncertain inverse problem method considering correlations for structural parameter identification, Structural and Multidisciplinary Optimization, 64 (2021) 1327-1342.

[38] H. Ouyang, J. Liu, Z. Li, X. Han, A novel dynamic model updating method for composite laminate structures considering non-probabilistic uncertainties and correlations, Composite Structures, 287 (2022) 115359.

[39] Y. Liu, L. Wang, K. Gu, A support vector regression (SVR)-based method for dynamic load identification using heterogeneous responses under interval uncertainties, Applied Soft Computing, 110 (2021) 107599.

[40] Y. Liu, L. Wang, K. Gu, M. Li, Artificial Neural Network (ANN)-Bayesian Probability Framework (BPF) based method of dynamic force reconstruction under multi-source uncertainties, Knowledge-Based Systems, 237 (2022) 107796.

[41] M. Faes, M. Broggi, E. Patelli, Y. Govers, J. Mottershead, M. Beer, D. Moens, A multivariate interval approach for inverse uncertainty quantification with limited experimental data, Mechanical Systems and Signal Processing, 118 (2019) 534-548.

[42] S. Bi, K. He, Y. Zhao, D. Moens, M. Beer, J. Zhang, Towards the NASA UQ Challenge 2019: Systematically forward and inverse approaches for uncertainty propagation and quantification, Mechanical Systems and Signal Processing, 165 (2022) 108387.

[43] A. Der Kiureghian, O. Ditlevsen, Aleatory or epistemic? Does it matter?, Structural safety, 31 (2009) 105-112.

[44] G. Li, S.-W. Wang, C. Rosenthal, H. Rabitz, High dimensional model representations generated from low dimensional data samples. I. mp-Cut-HDMR, Journal of Mathematical Chemistry, 30 (2001) 1-30.

[45] S. Rahman, H. Xu, A univariate dimension-reduction method for multi-dimensional integration in stochastic mechanics, Probabilistic Engineering Mechanics, 19 (2004) 393-408.

[46] S. Shan, G.G. Wang, Survey of modeling and optimization strategies to solve high-dimensional design problems with computationally-expensive black-box functions, Structural and multidisciplinary optimization, 41 (2010) 219-241.

[47] J.L. Wu, Y.Q. Zhang, L.P. Chen, Z. Luo, A Chebyshev interval method for nonlinear dynamic systems under uncertainty, Applied Mathematical Modelling, 37 (2013) 4578-4591.

[48] L. Wang, C. Xiong, J.X. Hu, X.J. Wang, Z.P. Qiu, Sequential multidisciplinary design optimization and reliability analysis under interval uncertainty, Aerospace Science and

Technology, 80 (2018) 508-519.

[49] Y. Chen, P. Logan, P. Avitabile, J. Dodson, Non-Model Based Expansion from Limited Points to an Augmented Set of Points Using Chebyshev Polynomials, Experimental Techniques, 43 (2019) 521-543.

[50] D. Moens, D. Vandepitte, Interval sensitivity theory and its application to frequency response envelope analysis of uncertain structures, Computer methods in applied mechanics and engineering, 196 (2007) 2486-2496.

[51] Y. Ni, Y. Xia, W. Liao, J. Ko, Technology innovation in developing the structural health monitoring system for Guangzhou New TV Tower, Structural Control and Health Monitoring: The Official Journal of the International Association for Structural Control and Monitoring and of the European Association for the Control of Structures, 16 (2009) 73-98.

[52] Y. Ni, Y. Xia, W. Lin, W. Chen, J. Ko, SHM benchmark for high-rise structures: a reduced-order finite element model and field measurement data, 10(4-5)(2012) 411-426.

[53] T.C. Truong, S. Cho, C.B. Yun, H. Sohn, Finite element model updating of Canton Tower using regularization technique, Smart Structures and Systems, 10 (2012) 459-470.

[54] S. Weng, Y. Xia, X.-Q. Zhou, Y.-L. Xu, H.-P. Zhu, Inverse substructure method for model updating of structures, Journal of Sound and Vibration, 331 (2012) 5449-5468.

[55] W.J.Yan, D. Chronopoulos, K.V. Yuen, Y.C. Zhu, Structural anomaly detection based on probabilistic distance measures of transmissibility function and statistical threshold selection scheme. Mechanical Systems and Signal Processing, 162 (2022)108009.